https://mof4air.eu

MOF4AIR

Metal Organic Frameworks for carbon dioxide Adsorption processes in power production and energy Intensive industRies

This project has received funding from the European Union's Horizon 2020 research and innovation programme under grant agreement No. 837975 (MOF4AIR).

Deliverable Report

Start date of project:	01/07/2019
Duration of project:	48 months
Deliverable nº & name:	D5.2: First results from testing of MOF in VPSA based adsorbents for post-combustion CO_2 capture at TRL 5 Original title: Main results from testing of MOF in VSA and MBTSAent
Version	1
Work Package n°	5
Due date of D:	31/03/2022
Actual date of D:	27/04/2023
Participant responsible:	UMONS
Main authors:	Arnaud Henrotin, Nicolas Heymans, Guy De Weireld
Website:	https://www.mof4air.eu/

Nature of the Deliverable		
R	Document, report (excluding the periodic and final reports)	R
DEM	Demonstrator, pilot, prototype, plan designs	
DEC	Websites, patents filing, press & media actions, videos, etc.	
OTHER	Software, technical diagram, etc.	

Dissemination Level		
PU	Public, fully open, e.g. web	
CO	Confidential, restricted under conditions set out in Model Grant Agreement	X
CI	Classified, information as referred to in Commission Decision 2001/844/EC	

Quality procedure			
Date	Version	Reviewers	Comments
23/03/2023	1	Marie-Eve Duprez (UMONS)	General review
19-20/04/2023	1	Marie-Eve Duprez (UMONS)	Review

PROJECT SUMMARY

This report is part of the deliverables from the project "MOF4AIR" which has received funding from the European Union's Horizon 2020 research and innovation program under grant agreement No 837975.

Power supply and carbon-intensive industries account for a large share of CO_2 emissions. Shifting towards a low-carbon economy requires cost-effective carbon capture solutions to be developed, tested, and deployed. Current solutions do not offer sufficient performance. Adsorption processes are promising alternatives for capturing CO_2 from power plants and other energy-intensive industries such as cement, steel, or petrochemical industries. In this regard, Metal Organic Frameworks (MOFs) are a widely studied class of porous adsorbents that offer tremendous potential, owing to their large CO_2 adsorption capacity and high CO_2 affinity. However, the performances of MOF-based carbon capture technologies have not been fully evaluated. MOF4AIR gathers 14 partners from 8 countries to develop and demonstrate the performances of MOF-based CO_2 capture technologies in power plants and energy-intensive industries. MOF4AIR aims to foster the uptake of CCS technologies by providing a TRL6-reliable solution matching end users' needs, notably by cutting the CCS energy penalty by more than 10%. The solutions developed will be highly replicable thanks to the consideration of a wide range of carbon-intensive sectors and clusters, notably through the project's Industrial Cluster Board.

More information on the project can be found at https://mof4air.eu.

OBJECTIVE AND EXECUTIVE SUMMARY

The main objective of the WP5 is the testing of the chosen shaped MOF adsorbents in lab scale pilot VPSA and MBTSA reactors to validate both reactor and process models developed in WP4. The testing will further give necessary knowhow on the design needed for the demonstration process to be developed in WP6.

WP5 is divided in three tasks:

- Task 5.1: Production and shaping of adsorbents for testing at TRL 5;
- Task 5.2: Prototypes and tests in a simulated relevant environment;
- Task 5.3: Recommendations for process upscaling.

This deliverable is related to Task 5.2. The original task has been divided in two sub-tasks: one concerning the VPSA testing at UMONS and the other one related to MBTSA testing at SINTEF. Task 5.2 will lead to two deliverables instead of one as initially planned:

- D5.2 “First results from testing of MOF in VPSA based adsorbents for post-combustion CO_2 capture at TRL 5” (This deliverable). It describes the VPSA prototype built at UMONS, the testing protocols used, the different tested configurations and the main results obtained for the first selected promising MOFs from WP3, MIL-160(Al), to prove the feasibility of the VPSA process, to provide data/refine models from T4.3 and to provide inputs for industrial demonstration sites.
- D5.5 (new deliverable) “Detailed results from testing of MOFs in VPSA and MBTSA based adsorbents for post-combustion CO_2 capture at TRL 5” will detail the results for both processes and will include a second adsorbent, MIL-120(Al), synthesized at medium scale from T5.1.

TABLE OF CONTENTS

LIST OF FIGURES

LIST OF TABLES

NOMENCLATURE

c_p	Isobaric heat capacity of the gas [J.mol^{-1}.K^{-1}]
D	Diameter of pipe [m]
d_p	Diameter of particle [m]
d_v	Diameter of the valve [inch]
ε	Bed void fraction [/]
ϵ	Surface roughness [m]
f	Friction factor of pipe [/]
g	Gravitational acceleration (=9.81 [m.s^{-2}])
K	Pressure drop coefficient [/]
L	Length of pipe [m]
M_w	Molecular weight [mmol.g^{-1}]
m_{ads}	Mass of adsorbent [g]
μ	Dynamic viscosity [Pa.s]
p	Pressure [Pa or bar]
$\bar{p}$	Mean pressure for pressure drop calculation [Pa]
Q	Flow rate [Nm^3.h^{-1} or NL.min^{-1}]
q	Adsorbed amount [mmol.g^{-1}]
R	Perfect gas law constant (=8.314 [J.mol^{-1}.K^{-1}])
ρ	Density [kg.m^{-3}]
S_p	Pumping speed [m^3.s^{-1}]
T	Temperature [°C or K]
V	Volume [m^3 or L]
v	Speed of gas [m.s^{-1}]
y	Gas molar fraction [/]

1 INTRODUCTION

This deliverable aims to test the shaped MOFs in an industrial-like environment at laboratory scale and validate the performance of VPSA process using MOFs for CO_2 capture from industrial flue gases. In Task 2.1, 17 MOFs were synthetized and characterized at 10 g scale. Based on the results obtained at this scale, 7 MOFs have been selected and synthetized at 100 g scale with different binders (see D3.2). MIL-160(Al) was selected for its good selectivity (30-35) of CO_2 over N_2, its moderate heat of adsorption (32-33 kJ/mol), and its stability against water. The performance of this MOF in a VPSA process was studied by simulation in D4.3, confirming the potential of this MOF for CO_2 capture in an industrial process. Based on the results described in previous deliverables (D3.2 and D4.3), MIL-160(Al) was the first selected MOF to be produced at 3-5 kg scale.

To confirm the simulation results, a VPSA lab-pilot was designed and assembled at UMONS to test the upscaled MOFs. This installation can perform and assess three different VPSA cycles *i.e.* 2-bed 5-step, 3-bed 5-step, and 3-bed 6-step, with a feed flow rate up to 1.5 $Nm^3.h^{-1}$ with different CO_2 concentration. The VPSA pilot is fully instrumented allowing to record temperature, pressure, flow rate and CO_2 concentrations for comparison with simulations.

Three samples of MIL-160(Al) were tested in the VPSA lab-pilot: (i) a batch of 3 kg produced by MOFTECH (Task 5.1), (ii) a batch of 60 kg produced by MOFTECH for use in TCM industrial pilot (Task 6.1), (iii) a batch of 50 kg produced by KRICT for use in Tüpraş industrial pilot (Task 6.1). For each MOF, pure component adsorption isotherms and breakthrough curve measurements were made to verify the adsorption capacity of the different samples. The materials were then tested in operating conditions with a 3-bed 6-step cycle (the sole configuration allowing to reach good performances in terms of recovery and purity according to the simulations performed previously (see D4.3)) to study the impact of several operating parameters (adsorption time, purge time and flow rate, light blowdown time and pressure, …), and to find the optimum conditions allowing to reach at least 90% of recovery and 95% of purity.

2 VACUUM PRESSURE SWING ADSORPTION (VPSA)

2.1 SIZING OF THE VPSA PILOT

The vacuum pressure swing adsorption (VPSA) pilot developed at UMONS was designed to treat around 0.5-1.5 $Nm^3.h^{-1}$ of gas containing 5-15% of CO_2 and 85-95% of N_2, with a bed volume around 1.1 L (per bed). The choice of equipment (vacuum pump, compressor, flowmeters, pipping, …) was made accordingly to those specifications. Moreover, the design of the VPSA pilot was made to perform tests in three different configurations: 2-bed 5-step, 3-bed 5-step and 3-bed 6-step (see D4.3 for complete description).

The first step of the pilot sizing was the determination of the piping diameter that should be used based on the pressure drop in the installation. For an ideal gas, the pressure drop in piping and equipment is given by equation (1):

$$p_1^2 - p_2^2 = v^2 \frac{\overline{p^2} M_w}{RT} \left[\frac{4fL}{D} + 2\ln\left(\frac{p_1}{p_2}\right) + \sum K\right] \quad (1)$$

This equation takes into account the pressure drop due to the piping friction $\left(\frac{4fL}{D}\right)$, the pressure change caused by acceleration of gas as its density decreases $\left(2\ln\left(\frac{p_1}{p_2}\right)\right)$ and the pressure drop in the piping elements $(\sum K)$ [1]. The frictional factor (f) was computed with the Churchill equation [2] given by equations (2) to (5):

$$f = 2\left[\left(\frac{8}{Re}\right)^{12} + \frac{1}{(A+B)^{\frac{3}{2}}}\right]^{\frac{1}{12}} \quad (2)$$

$$A = \left[2.457\, ln \frac{1}{\left(\frac{7}{Re}\right)^{0.9} + 0.27\frac{\epsilon}{D}}\right]^{16} \quad (3)$$

$$B = \left(\frac{37530}{Re}\right)^{16} \quad (4)$$

$$Re = \frac{v\, D\, \rho}{\mu} \quad (5)$$

The value of surface roughness (ϵ) was taken equal to 0.0457 mm which is a typical value for commercial steel [1]. The values of K were obtained from literature data [1], [3]. For valves, factor K was determined based on flow coefficient (C_v) provided by manufacturer. The relation between K and C_v is given by equation (6).

$$C_v = \frac{29.9 d_v^2}{\sqrt{K}} \quad (6)$$

The pressure drop inside the adsorption column was determined by the Ergun equation [4] given by equation (7). In addition, the change of pressure due to the gas ascension was computed by the Bernoulli equation (8) assuming a vertical adsorption column with the gas flowing from bottom to top [1].

$$\Delta p = \frac{150\mu L}{d_p^2}\frac{(1-\varepsilon)^2}{\varepsilon^3} v + \frac{1{,}75 L\rho}{d_p}\frac{(1-\varepsilon)}{\varepsilon^3} v^2 \quad (7)$$

$$p_1 + \rho_1 g z_1 + \frac{\rho_1 v_1^2}{2} = p_2 + \rho_2 g z_2 + \frac{\rho_2 v_2^2}{2} + \Delta p \quad (8)$$

This set of equations was solved to determine the total pressure drop of the installation. A mixture of 15% CO_2 and 85% N_2 at 20°C and 2 bar was considered for the computation of the initial gas density and viscosity. The initial design of the pilot used for the pressure drop calculation contained 10 m of pipes, four 90° ells, two gate valves, two diaphragm valves, and three 3-way valves. The adsorption column considered contains spherical adsorbent of 1 mm diameter (minimum size of shaped MOF used) with a bed porosity of 0.4.

The pressure drop was calculated for three pipe diameters (1/4", 3/8" and 1/2") with a flow rate ranging from 0 to 1.5 $Nm^3.h^{-1}$. The results obtained are presented in Figure 1.

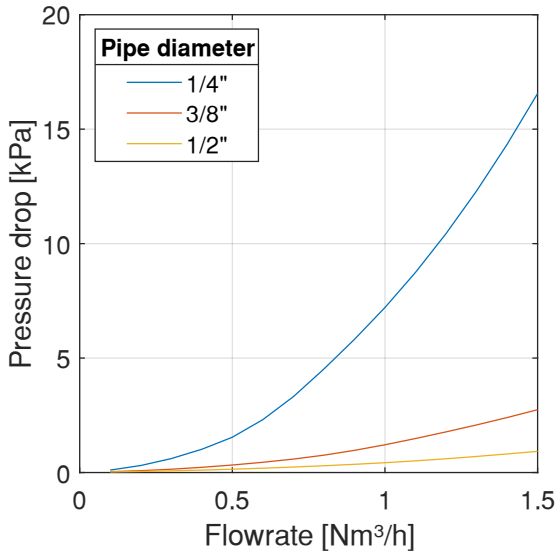

Figure 1: Pressure drop versus flow rate for different pipe diameters.

Results obtained show a higher pressure drop for the 1/4" pipes, more specifically above 1 $Nm^3.h^{-1}$. The 3/8" pipes allow a significant pressure drop reduction and operate the VPSA pilot at higher flow rate. Moreover, the total length of pipes and the number of elements was underestimated since this pressure drop calculation was a first estimation, and the P&ID of the pilot was not finalized yet. A diameter of 3/8" was therefore chosen as a compromise according to the calculations. A diameter of 1/2" would have led to a higher dead volume in the pipes, and an increase of the costs of the pilot.

The sizing of the vacuum pump was based on the characteristic curve of the pump and the characteristics of the piping in the VPSA pilot. A total length of 2 meters was taken for the calculations, in addition with 2 solenoid valves, 3 manuals valves, and a 90° elbow. The pumping time of a volume V vessel from a pressure p_i to a pressure p is given by equation (9) for a constant pumping speed S_p [5].

$$t = \frac{V}{E}\left[\frac{1}{p} - \frac{1}{p_i}\right] + \frac{V}{S_P}\left\{\frac{\left[\left(\frac{S_P}{E}\right)^2 + p^2\right]^{\frac{1}{2}}}{p} - \frac{\left[\left(\frac{S_P}{E}\right)^2 + p_i^2\right]^{\frac{1}{2}}}{p_i}\right\} + \frac{V}{S_P}\left\{\ln\frac{p_i + \left[\left(\frac{S_P}{E}\right)^2 + p_i^2\right]^{\frac{1}{2}}}{p + \left[\left(\frac{S_P}{E}\right)^2 + p^2\right]^{\frac{1}{2}}}\right\} \quad (9)$$

Since the pumping speed is not constant and depends on the pressure at the inlet of the vacuum pump, equation (9) was solved for small pressure differences ($p - p_i$), and the total pumping time was obtained by summing the pumping times for each small differences of pressure.

The E factor of equation (9) is obtained by equation (10) and depends on the length and diameter of pipe. To consider the other elements of the piping, an equivalent length can be computed from the factor K by equation (11).

$$E = \frac{\pi D^4}{128 \mu L} \tag{10}$$

$$L = \frac{KD}{4f} \tag{11}$$

Several pumps available on the market were compared based on the pumping time needed to reach a pressure of 0.1 bar from 1 bar on the empty adsorption bed. Results obtained are shown in Figure 2.

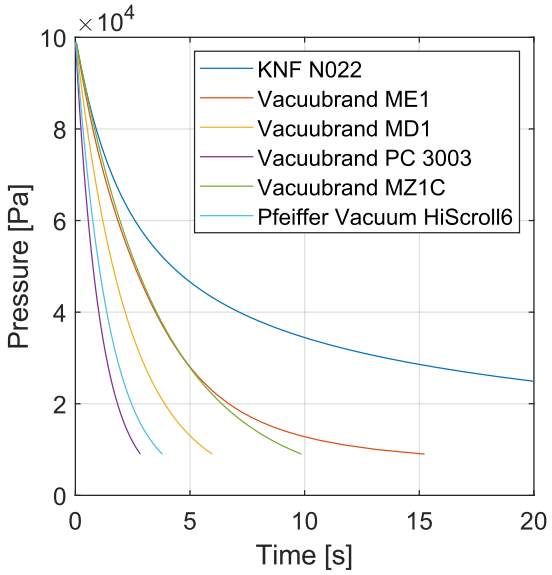

Figure 2: Pumping time obtained for different vacuum pumps.

The best results were obtained with the Vacuubrand PC 3003 (2.7 s) and the Pfeiffer Vacuum HiScroll6 (3.6 s). In this calculation, the gas desorption from the adsorbent is not considered. The calculation of the gas volume of gas adsorbed depends on the adsorbent, and the speed of desorption can be complex to model. The pumping times obtained should probably be multiplied by 5 to 10 to consider the gas desorption. The HiScroll6 was selected due to the automation capacity of the vacuum pump and on economic basis.

The flowmeters and the compressor of the VPSA pilot were chosen in accordance with the feed flow rate (0.5-1.5 $Nm^3.h^{-1}$) and the first simulation results. At the column outlet, the flow rate can reach the same value as the feed flow rate. For the blowdown step, the flow rate depends on the sizing of the vacuum pump and the desorption rate of the adsorbent. The purge and rinse flow rates are lower than the feed flow rate since the purge is part of the flow rate coming from the outlet of the adsorption column. The compressor is sized based on the maximum rinse flow rate (20 $NL.min^{-1}$), with an outlet pressure of 2.5 bar, to perform VPSA cycle with a maximum adsorption pressure of 2 bar.

2.2 DESCRIPTION OF VPSA LABORATORY PILOT

The VPSA pilot developed at UMONS aims to reproduce the behavior of an industrial VPSA pilot at the scale of 1 $Nm^3.h^{-1}$ of flue gas. The pilot comprises a gas generation system, three adsorption beds, a vacuum pump, and a compressor, allowing the operation in three different configurations: 2-bed 5-step, 3-bed 5-step, and 3-bed 6-step (see D4.3 for complete description). The VPSA pilot is also fully instrumented, providing measurements of temperature, pressure, gas composition, and flow rate at various key points. The complete P&ID of the VPSA pilot developed for the MOF4AIR project is given in Figure 18 in Appendix. For the ease of representation and explanation, the complete P&ID was divided into five sections: Feed, Columns, Waste, Product, and Analyzer.

2.2.1 FEED SECTION

This section is dedicated to the generation of the gas mixture and its analysis. The detailed feed section is presented in Figure 3. The CO_2/N_2 gas mixture is generated by two thermal mass flow controllers from Bronkhorst. In addition, a Coriolis mass flow controller and an evaporator are present to inject water vapor into the gas mixture. The three flow controllers are connected with ¼ inch pipes and can be isolated with manual valves to perform a zeroing procedure. The distance between the flowmeters and the valves is equal to ten times the piping diameter (6.5 cm) to avoid disruption of the flow. CO_2 and N_2 come from gas cylinders with a purity higher than 99.999% (Air Liquide). The water comes from liquid demineralized water tank under pressure (3 bar). The specifications of the three flow controllers are:

- Nitrogen: F-201AV from Bronkhorst with a full-scale of 0.06 to 3 $Nm^3.h^{-1}$;
- CO_2: F-201AV from Bronkhorst with a range of 0.02 to 1 $Nm^3.h^{-1}$;
- Water: M12-RGF from Bronkhorst with a range of 2.32 to 116 $g.h^{-1}$;
- Evaporator: W-303B-220-K from Bronkhorst with a water range of 20 to 1120 $g.h^{-1}$ and gas range of 5 to 100 $NL.min^{-1}$.

At the outlet of the evaporator, the pipe diameter is enlarged to 3/8 inch for the rest of the installation. A ¼ inch solenoid valve (VA1: Asco 262 with an opening of 2.4 mm and K_v of 0.15 $m^3.h^{-1}$) allows the gas to be sent to the gas analyzer for feed composition analysis. This valve is normally closed during VPSA cycle. Further along the line, two manual valves allow to isolate the feed section of the columns, and to vent the piping in case of maintenance.

A flow meter (SLA5860 from Brooks with a full-scale of 1.5 $Nm^3.h^{-1}$ and calibrated for 15% CO_2 / 85% N_2) allows the measurement of the gas mixture total flow rate and the check that the generated flow matches the desired flow. As for the flow controllers, the distance between flow meter and valves is equal to ten times the diameter of the pipping (10 cm) to avoid flow disruptions. This rule has been applied to all flowmeters of the installation.

Then, the gas flows through a proportional valve (VP1: Asco 202 with an opening of 4 mm and K_v of 0.42 $m^3.h^{-1}$) which can be modulated for pressurization steps. Before the columns section, a pressure transmitter (Retec ATMECO with a range of 0-5 bar abs) is placed to measure the pressure before the adsorption beds.

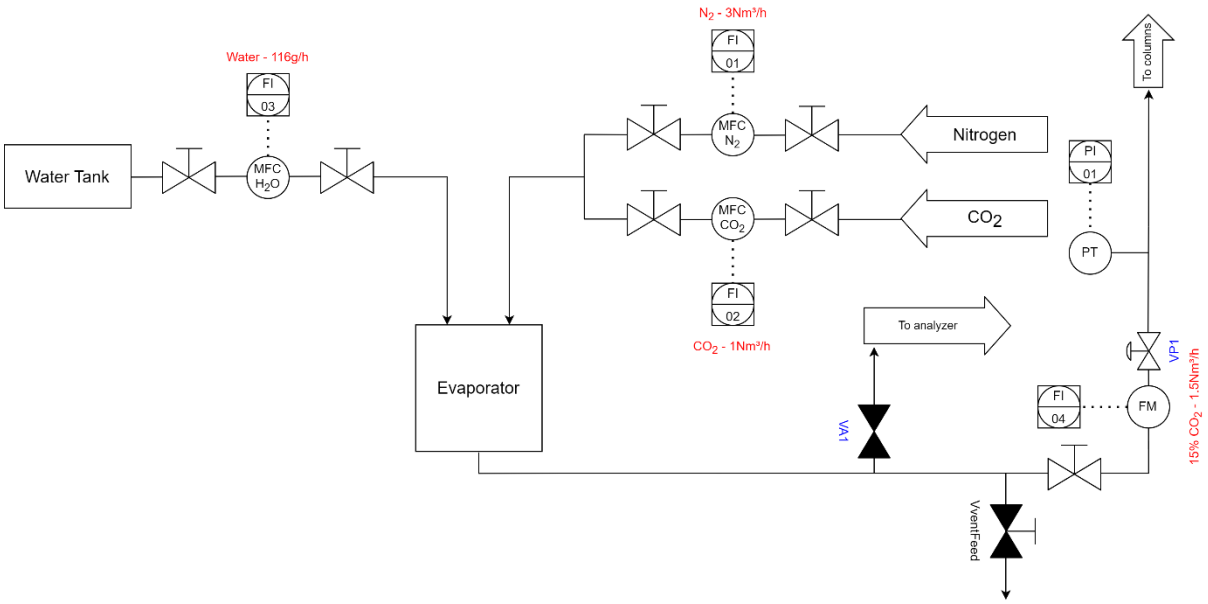

Figure 3: Feed section of the VPSA pilot.

2.2.2 COLUMNS SECTION

The columns section is the central part of the VPSA pilot and is represented in Figure 4. This section contains 19 valves (V1 to V19: Asco 263 with an opening of 4 mm and K_v of 0.45 $m^3.h^{-1}$) allowing to direct the gas flow to the different sections of the installation. Valves V1, V4, and V7 connect the feed section to the bottom of the three adsorption beds. Valves V2, V5 and V8 connect the bottom of the beds to the product section for blowdown and purge steps, and valves V3, V6, and V9 connect the product section to the bottom of beds for rinse step. At the top of the adsorption beds, V13, V16 and V19 connect the beds to the waste section, and V12, V15, and V18 connect the waste section to beds for purge and pressurization steps (only in 3-bed 6-step configuration). V11, V14 and V17 connect the beds to the product section for light blowdown step. A 3-way valve (V3V2: Asco 327 with an opening of 5.7 mm and K_v of 0.45 $m^3.h^{-1}$) allows to switch between top or bottom of the adsorption beds. The valve V10 is used for pressure equalization steps during the 2-bed 5-step cycle.

The three adsorption columns have a length of 30 cm and a diameter of 7.01 cm giving and L/D ratio of 4.28. A filler piece can be used in the columns to reduce the length to 20 cm. A filter at the bottom and top of the columns retains the adsorbent in the column and evenly distributes the gas. Each adsorption bed is equipped with a temperature sensor (type K thermocouple) at the inlet and the outlet of the bed. Column 1 is equipped with an immersion sleeve to measure the temperature inside the column (Type K thermocouple) at 5 cm and 25 cm starting from the bottom of the adsorption layer. Columns 2 and 3 can

be isolated with manual valves to work with one (breakthrough curves) or two columns (2-bed 5-step configuration).

At the outlet of the columns a pressure transmitter (Retec ATMECO with a range of 0-5 bar abs) measures the pressure drop inside the adsorption beds. The two flowmeters before waste and product sections are explained in their respective sections.

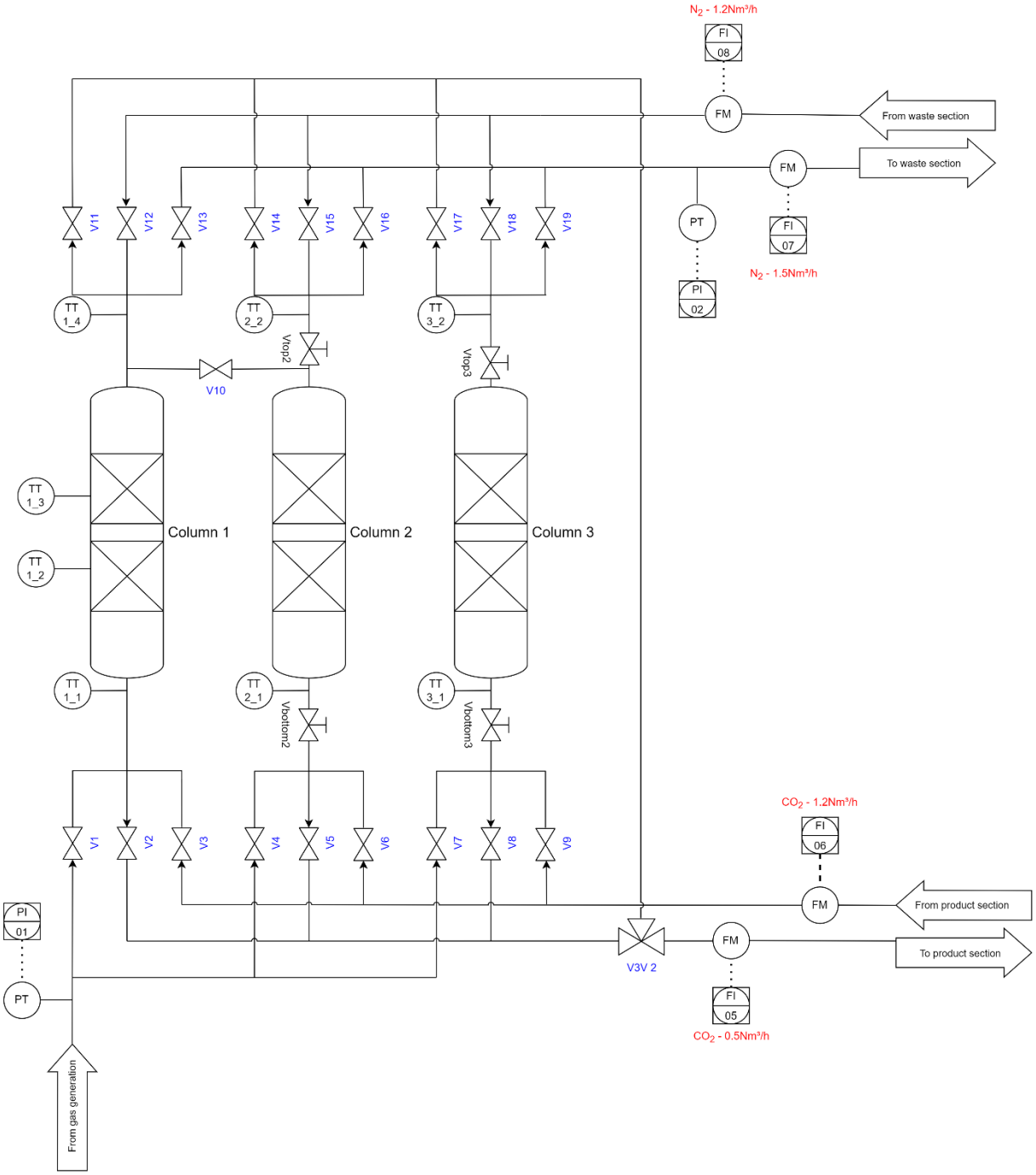

Figure 4: Columns section of the VPSA pilot.

2.2.3 WASTE SECTION

The waste section is connected to the top of the adsorption beds and contains nitrogen-rich streams. This section is also dedicated to the purge step. Waste section P&ID is represented in Figure 5.

From the columns, the flow is first measured with a flowmeter (SLA5860 from Brooks with a full-scale of 1.5 $Nm^3.h^{-1}$ and calibrated for 100% N_2) before the check valve and valve V24. The valve V24 (Asco 262 with an opening of 2.4 mm and K_v of 0.15 $m^3.h^{-1}$) allows to use a part of the flow rate from the columns for the purge via the flow controller (SLA5850 from Brooks with a full-scale of 1.2 $Nm^3.h^{-1}$ and calibrated for 100% N_2). In this case, the valve V25 (Asco 263 with an opening of 4 mm and K_v of 0.45 $m^3.h^{-1}$) is closed. The purge can be done with the gas contained in the nitrogen tank by opening V25 and closing V24.

The nitrogen tank used in this section has a total volume of 500 L and receives the flow rate from the outlet of the column (bottom left of the tank on Figure 5). Before the tank, a valve (VA2: Asco 262 with an opening of 2.4mm and K_v of 0.15 $m^3.h^{-1}$) allows the flow analysis. The tank is equipped with a temperature sensor (Pt100), and a pressure transmitter (Retec ATMECO with a range of 0-5 bar abs). The tank has two outlets, the first one is located on the upper left of the tank on the P&ID and is used for purge. The second one is located on the upper right, this outlet is connected to the analyzer, and a back pressure controller (5866RC from Brooks with a full-scale of 1 $Nm^3.h^{-1}$ and calibrated for 100% N_2). This controller allows keeping a constant pressure in the nitrogen tank thus setting the adsorption pressure of the VPSA process. The bottom right of the tank is connected to the outlet of the analyzer, making an analyzing loop of the tank from the upper right outlet.

Several manual valves are placed on the P&ID to isolate the nitrogen tank for maintenance and start-up. The tank is connected to an inlet (at the bottom), allowing to purge the tank, and fill it with pure nitrogen.

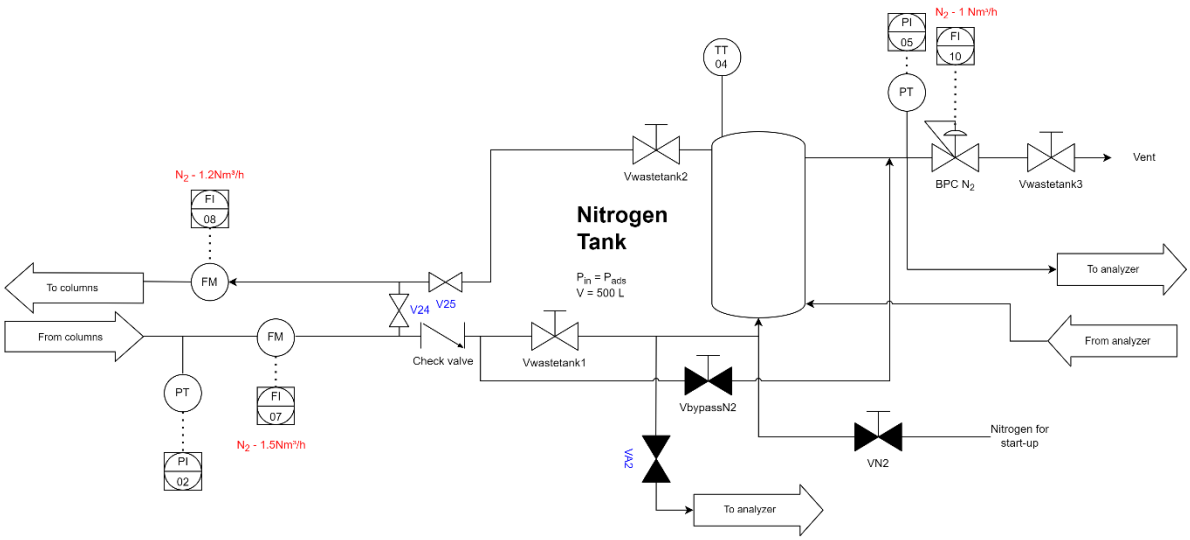

Figure 5: Waste section of the VPSA pilot.

2.2.4 PRODUCT SECTION

Product section is similar to the waste section of the pilot and is dedicated to the blowdown and rinse steps. As for the waste section, it contains a tank storing the CO_2 retrieved from the adsorbent. The P&ID of this section is represented in Figure 7.

From the columns section, a flowmeter (SLA5860 from Brooks with a full-scale of 0.5 $Nm^3.h^{-1}$ and calibrated for 100% CO_2) is used, followed by a Pirani gauge for pressure measurement under vacuum (CMR 361 from Pfeiffer Vacuum with a range of 0.1 to 1100 mbar), and a proportional valve (VP2: Asco 202 with an opening of 4 mm and K_v of 0.42 $m^3.h^{-1}$). This valve is used to regulate the pressure during the blowdown steps based on the measurement of the Pirani gauge. A 3-way valve (Asco 327 with an opening of 5.7 mm and K_v of 0.45 $m^3.h^{-1}$) is used to bypass the vacuum pump when the pressure is higher than the CO_2 tank pressure. Two check valves are used to avoid back-flow from the vacuum pump and the bypass line. The vacuum pump used is the HiScroll 6 from Pfeiffer Vacuum. This pump is dry and oil-free to avoid contaminants in the adsorption columns and has a pumping speed of 6.1 $m^3.h^{-1}$ at atmospheric pressure, and a typical lowest pressure of 2 Pa. The speed of the pump can be adjusted via numerical communication, allowing to reduce the speed during the light blowdown step to reach a set-up pressure value. The flow curve of the pump is given in Figure 19 in Appendix.

To regulate and maintain a pressure setpoint during blowdown and purge steps, a PID controller is used to control the opening of valve VP2 according to the pressure measurement and setpoint. The controller parameters were found with the Ziegler–Nichols method [6]: a constant flow of nitrogen is sent by the top of the column, and the vacuum pump is connected to the bottom (see Figure 6). The first step of the tuning method is to set the integral and derivative terms to 0, and increase the proportional term until the critical gain is reached (*i.e.* consistent oscillation is observed in the response of the controller). From the critical gain value and the period of oscillation, the parameters of the PID can be calculated, and eventually adjusted.

The same experiment was performed for the light blowdown step to keep a higher pressure in the adsorption column (0.4 to 0.8 bar). To avoid overshoot due to the speed of the vacuum pump, the speed of the pump was reduced to 40%, and the opening of the regulation valve was limited to 60%. Parameters obtained with these conditions are slightly different and given in Table 1.

Table 1: Parameters obtained from PID tuning.

	Blowdown and purge	**Light blowdown**
Proportional constant	-180	-120
Integral time [ms]	20	1050
Derivative time [ms]	5	262.5

After the vacuum pump, several solenoid valves allow the flow control according to the stages. The valve VA3 (Asco 262 with an opening of 2.4 mm and K_v of 0.15 $m^3.h^{-1}$) allows the flow analysis during the blowdown step. Valves V22 and VA4 (Asco 262 with an opening of 2.4 mm and K_v of 0.15 $m^3.h^{-1}$) are used during the light blowdown step, V22 leads to the atmosphere, and VA4 leads to the analyzer. V20, V21 and V23 (Asco 263 with an opening of 4 mm and K_v of 0.45 $m^3.h^{-1}$) are used during blowdown and rinse steps. Valve V21 is opened only during the blowdown step. During this step V20 and V23 are closed. During the

rinse step, the rinse flow can come directly from the columns, in this case, V21 and V23 are closed and V20 is opened. If the rinse flow comes from the CO_2 tank, V20 is closed and V23 is opened.

The CO_2 tank configuration is like the nitrogen tank from waste section. The gas from the columns enters by the lower left inlet and exits the tank by the upper left or right outlets. The left outlet is dedicated to the rinse step, and the right outlet is connected to the gas analyzer and a back pressure controller (5866RC from Brooks with a full-scale of 0.2 $Nm^3.h^{-1}$ and calibrated for 100% CO_2). This controller allows to keep a constant pressure in the CO_2 tank. The lower right inlet of the tank is connected to the analyzer, making an analysis loop from the upper right outlet. The tank volume is 200 L and is equipped with a temperature sensor (Pt100) and a pressure transmitter (Retec ATMECO with a range of 0-5 bar abs). An inlet is also available for purge and filling of the tank.

The rinse flow rate is regulated with a flow controller (SLA5850 from Brooks with a full-scale of 1.2 $Nm^3.h^{-1}$ and calibrated for 100% CO_2) which is totally open when the rinse is generated with the flow from the columns (3-bed 6-step configuration). The rinse flow needs to be compressed since the adsorption columns are at higher pressure than the CO_2 tank. The compressor used for the rinse step is N922STE diaphragm pump from KNF. This pump allows to reach a maximum pressure of 5 bar (absolute), with a flow rate of 9.5 $L.min^{-1}$ at this pressure. At atmospheric pressure, the maximum flow rate is equal to 21 $L.min^{-1}$. The characteristic curve of this pump is given in Figure 20 (Appendix). A check valve is used at the outlet of the compressor to avoid backflow, a pressure transmitter (Retec ATMECO with a range of 0-5 bar abs) allows to measure the pressure generated by the compressor.

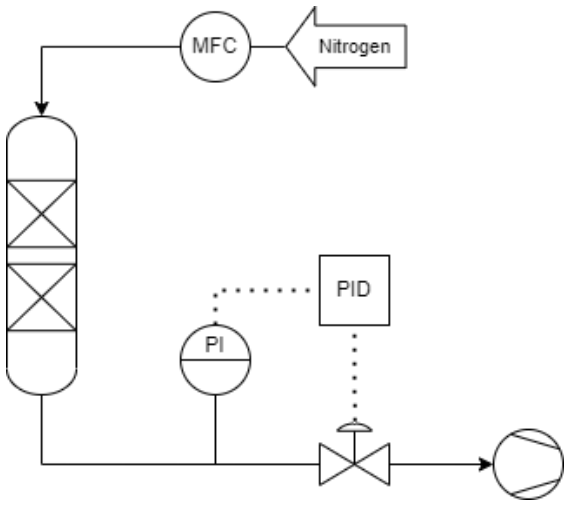

Figure 6: Set-up used for PID tuning.

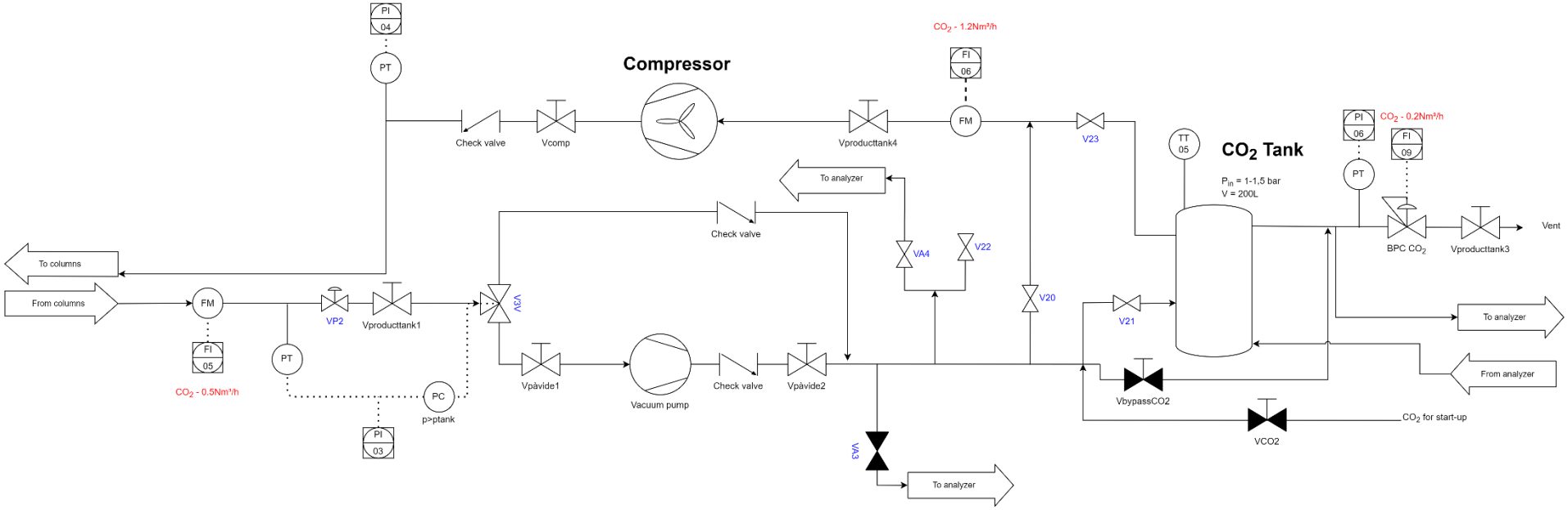

Figure 7: Product section of the VPSA pilot

2.2.5 ANALYZER SECTION

The gases are analyzed by a four-channel NDIR analyzer (Emerson X-STREAM Enhanced) with a measuring range of 0-100% CO_2. All the channels were calibrated with a 99.999% N_2 gas for zeroing. Channels one and two which are connected to the waste section and nitrogen tank were calibrated with a gas mixture containing 15% CO_2 / 85% N_2 with 2% of relative uncertainties on concentration. The two other channels were calibrated with 99.999% CO_2 gas. A correction based on the density of the analyzed gas must be applied on the value obtained from the analyzer. This correction is based on the pressure of the gas since the analyzer is maintained to 70°C. This correction is explained in Section 2.3.4.1.

Six sampling points exist on the pilot and are shown in Figure 8. Inlet and outlet of channel 1 are connected to the nitrogen tank, making a continuous analysis of the tank concentration. The circulation of the gas is assured by a pump (KNF NMP830 with a maximum flow rate of 3.1 L.min^{-1}) with a variable motor speed. The inlet of channel 2 is connected to the feed, waste, and product section (used during light blowdown step). The outlet of this channel can be connected to the atmosphere (VA5) or the nitrogen tank (VA6) by the opening of two solenoid valves (Asco 262 with an opening of 2.4 mm, K_v of 0.15 m^3.h^{-1}). Channel 3 comes from the product section and is used during blowdown or purge step. The channel 4 inlet is connected to the CO_2 tank. Both channel 3 and 4 outlets are connected to the CO_2 tank. As for channel 1, a circulation pump (KNF NMP830 with a maximum flow rate of 3.1 L.min^{-1}) is used for channel 4.

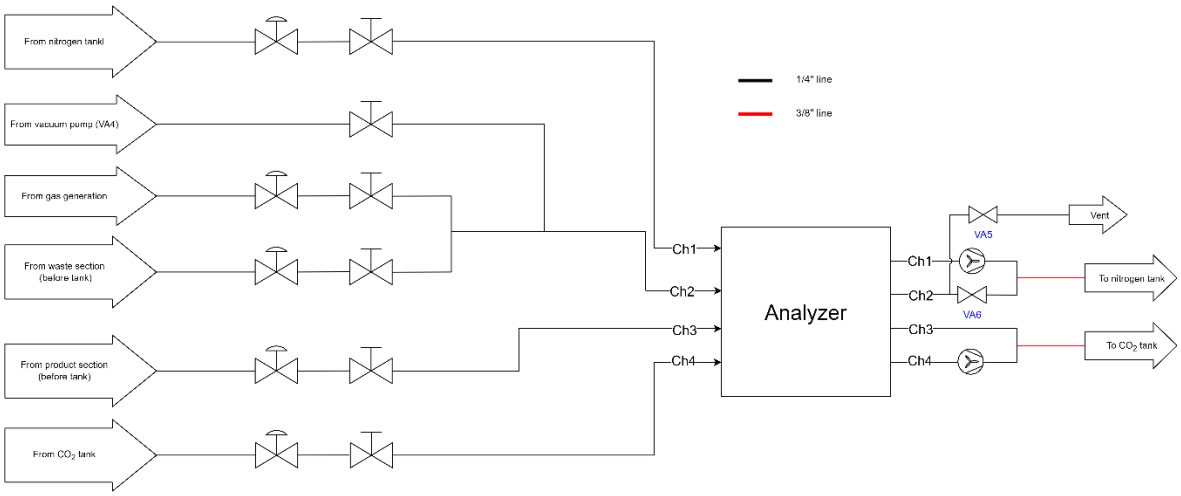

Figure 8: Analyzer section of the VPSA pilot.

2.2.6 DATA ACQUISITION AND CONTROL

The operating of the VPSA pilot is provided by a programmable logic controller (PFC100 from Wago), allowing to record temperature, pressure, flow rate, and gas concentration, to receive the different signals from the equipment, to record the data, and to control manually or automatically the installation. A home-made software was developed on e-cockpit (software provided by Wago) to allow communication between the elements of the pilot, and to provide a graphical user interface. The interface allows to control individually each component (valves, flow controllers, vacuum pump, compressor, …), but also to define the VPSA cycle to perform by giving the cycle parameters (see Figure 9).

The software developed allows to record temperature, pressure, flow, and concentration every seconds. During the operation of a cycle, purity and recovery are computed (see Section 2.3.4.3) from the flow and

concentration recorded to give the evolution of both indicators for each completion of a cycle, allowing to determine when the pilot is in steady state. In addition, the analysis procedure described in Section 2.3.2 and 2.3.3 are fully automated and can be run during or at the end of an experimental measurement.

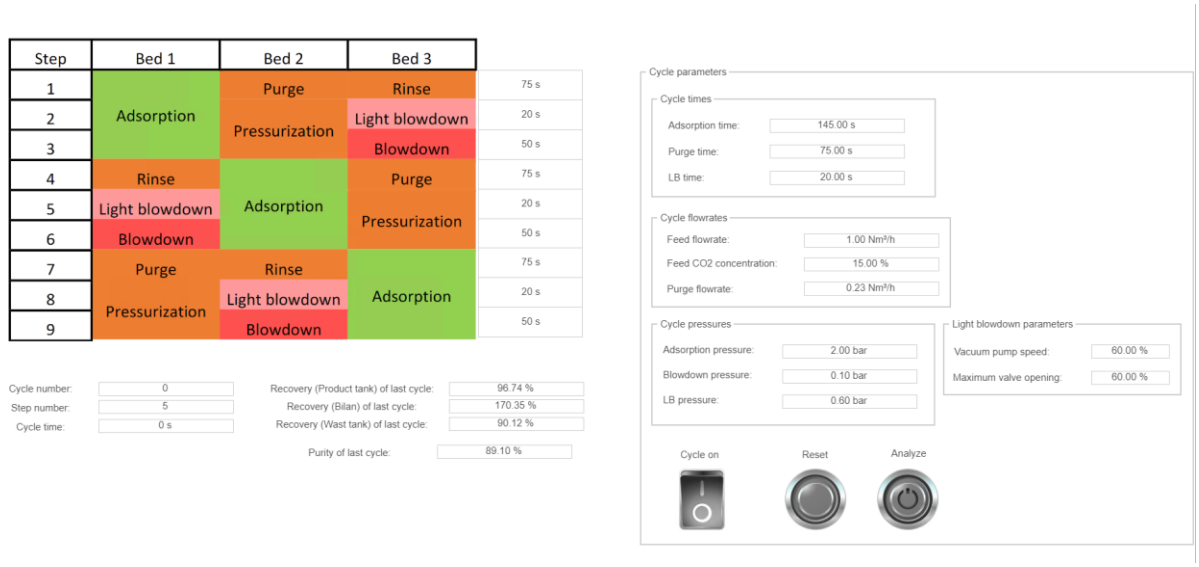

Figure 9: Graphical user interface for the configuration of the 3-bed 6-step cycle.

2.3 OPERATION OF THE PILOT

The pilot described in section 2.2 was tested with the 3-bed 5-step cycle and 3-bed 6-step cycle. This last cycle was tested with three samples of MIL-160(Al). The start-up procedure, the operation of the cycle, and the analysis of the results are described in this section.

2.3.1 START-UP PROCEDURE

Before the first test of VPSA cycle, or after a modification in the piping, the installation is flushed with nitrogen to avoid the adsorption of water or other compound contained in air. Nitrogen and CO_2 tanks were emptied with a vacuum pump and filled with pure nitrogen and CO_2 (>99.999%).

The adsorption columns were filled with adsorbent by filling slowly and shaking the columns to obtain a bulk density of adsorbents as high as possible. The same amount of adsorbent was used for the three columns to avoid acyclic phenomena. The adsorbent can be regenerated with a heating jacket during 24h (with a ramp of 1°C.min^{-1} and an outgassing temperature related to the adsorbent) under vacuum (typical lowest pressure of the vacuum pump: 2 Pa). The adsorption columns are then pressurized with nitrogen. The regeneration can be done only with vacuum without heating, or with pure nitrogen flow with or without heating, depending on the adsorbent and the conditions tested.

2.3.2 3-BED 5-STEP CYCLE

The 3-bed 5-step cycle was described in detail in D4.3. The different steps of the cycle are given in Table 2. This cycle was implemented and tested on the VPSA pilot allowing the testing of the different parameters of the cycle: adsorption time, purge time, rinse time, adsorption pressure, blowdown pressure, purge flow rate, and rinse flow rate.

The cycle is performed as follow: the gas mixture is generated within the feed section and is sent to the columns. The valves V1, V4, V7 are used to send the gas to the columns in adsorption step. The same valves are used for the pressurization step, splitting the feed gas into two columns. The gas exits then the column by the valve V13, V16 or V19 and goes to the waste section. The valves V24 and V25 of waste section are closed when no bed is in purge step. During a purge step, the valve V25 is opened, and a flow rate (from nitrogen tank) is set by the flow controller. The gas is then sent to the column in purge by the valve V12, V15 or V18. At the bottom of the column in purge step, the valve V2, V5 or V8 is open to send the gas to the product section. In product section, only the valve V21 is open to send the gas to the CO_2 tank.

During a blowdown step, the valve set is similar to the purge step, excepted for the valves at the top of the adsorption bed (V12, V15 or V18 is closed). During the rinse step, the valve V23 is opened to send the gas to the compressor. The flow controller of this section allows to set the rinse flow rate (from CO_2 tank). The valve V3, V6 or V9 is opened to receive the rinse flow rate, and the valve V13, V16 or V19 is also open. From a practical point of view, the time and the flow rate of the rinse step must be chosen in accordance with the feed flow rate to avoid sending more CO_2 than recovered during the blowdown, leading to negative recoveries, and a decrease of CO_2 tank pressure.

The complete valve set used for the 3-bed 5-step cycle is given in Table 7 in Appendix. During the cycle, the CO_2 concentration of both CO_2 and N_2 tanks are continuously analyzed by the analysis loop described in the section 2.2.5. In addition, the gas coming from the outlet of the adsorption columns is continuously analyzed via the valve VA2 from the waste section. In a similar way, the CO_2 concentration coming from the vacuum pump outlet is analyzed with the valve VA3.

Table 2: State of each bed during the 3-bed 5-step cycle.

<table>
<tr><th>Step</th><th>Bed 1</th><th>Bed 2</th><th>Bed 3</th></tr>
<tr><td rowspan="3">1</td><td rowspan="3">Adsorption</td><td>Blowdown</td><td>Rinse</td></tr>
<tr><td>Purge</td><td rowspan="3">Blowdown</td></tr>
<tr><td>Pressurization</td></tr>
<tr><td>2</td><td>Rinse</td><td rowspan="3">Adsorption</td></tr>
<tr><td rowspan="3">3</td><td rowspan="3">Blowdown</td><td>Purge</td></tr>
<tr><td>Pressurization</td></tr>
<tr><td>Rinse</td><td rowspan="3">Adsorption</td></tr>
<tr><td>4</td><td>Purge</td><td rowspan="2">Blowdown</td></tr>
<tr><td>5</td><td>Pressurization</td></tr>
</table>

2.3.3 3-BED 6-STEP CYCLE

The second configuration implemented in the VPSA pilot is the 3-bed 6-step cycle. More information on this cycle is available in D4.3. The state of each bed during the cycle is found in Table 3. This cycle is similar to the 3-bed 5-step with some modifications: the blowdown is split into two different steps, the light blowdown where the gas is sent to the atmosphere, and “classical” blowdown where the gas is retrieved and stored in the CO_2 tank. In addition, the purge is slightly modified to use directly the gas coming from the adsorption columns via the valve V20. Purge and rinse steps are linked in this cycle. The gas coming

from the bottom of the column in purge step is directly used for the rinse step instead of the gas from the CO_2 tank. The VPSA pilot allows the study of the following parameters: adsorption time, purge time, light blowdown time, purge flow rate, adsorption pressure, light blowdown pressure and blowdown pressure.

As the 3-bed 5-step cycle, the gas is generated in the feed section, and sent to the column in adsorption step via V1, V4 or V7, and the gas exits the column via V13, V16 or V19 to go to the waste section. In waste section, the valve V24 is opened if a bed is in purge step, allowing to use part of the gas coming from the bed in adsorption step. The purge flow rate is controlled by the flow controller of this section. The gas is then sent to the column in purge by the valve V12, V15 or V18. At the bottom of the column in purge step, the valve V2, V5 or V8 is open to send the gas to the product section. In product section during the purge/rinse step, the valves V21 and V23 are closed, and the valve V20 is open to directly use the purge flow for the rinse of another column. The flow controller used for rinse is fully opened (setpoint of 100%) and the compressor is turned on to send the rinse flow rate via V3, V6 or V9. The pressurization of a column is similar to the purge and is made by sending gas through the N_2 flow controller, except that the bottom of the column is not opened to increase the pressure to the adsorption pressure.

During the light blowdown step, the column is evacuated by the top to the product section by opening the valve V11, V14 or V17, and switching the 3-way valve V3V2. From a practical perspective, the light blowdown is divided into two parts: the evacuation from the adsorption pressure to atmospheric pressure, and the evacuation from atmospheric pressure to light blowdown pressure. The first part is made by switching the 3-way valve V3V1 to the bypass of vacuum pump and by opening the valve V22 for 10 seconds. After, the 3-way valve V3V1 is switched to the vacuum pump to decrease the pressure under atmospheric pressure. The speed of the pump is adjusted (motor speed is set between 40% and 80% depending on the pressure and the time of the light blowdown step) to avoid a decrease of pressure too fast.

The light blowdown is followed by the classical blowdown, which is made by the bottom of the column, via the valve V2, V5, or V8. The 3-way valve V3V2 is also switched, and the speed of the vacuum pump is set to 100%. After the vacuum pump, only the valve V21 is open to retrieve the CO_2 stream in the CO_2 tank.

The complete valve set used for the 3-bed 6-step cycle is given in Table 8 in the Appendix. During the cycle, the CO_2 concentration of both CO_2 and N_2 tanks is continuously analyzed by the analysis loop described in Section 2.2.5. Due to the complexity of the cycle, all flows cannot be analyzed simultaneously during one cycle. A procedure was developed to analyze the gas concentration at different locations in the pilot during each step. The procedure is as follows: first, the concentration of the flow coming out the columns is analyzed during a complete adsorption step on channel 2 of the analyzer via the valve VA2. It is to be noted that the flow coming out of the columns at the beginning of the adsorption step is composed of the rinse and adsorption flows (see Table 3). Then, the flow coming from the vacuum pump is analyzed during the light blowdown step via the valve VA4 on channel 2. During the blowdown step, the flow coming from the vacuum pump is analyzed on channel 3 via the valve VA3. The flow coming from the bottom of the columns during the purge step is also analyzed via the valve VA3. The valve V20 is closed during the analysis of the purge flow. The feed flow rate is then analyzed on channel 2 via the valve VA1 in the feed section.

Table 3: State of each bed during the 3-bed 6-step cycle.

Step	Bed 1	Bed 2	Bed 3
1	Adsorption	Purge	Rinse
		Pressurization	Light Blowdown
			Blowdown
2	Rinse	Adsorption	Purge
3	Light Blowdown		Pressurization
4	Blowdown		
5	Purge	Rinse	Adsorption
6	Pressurization	Light Blowdown	
		Blowdown	

2.3.4 RESULTS ANALYSIS

During the pilot operation, all the measurements (temperature, pressure, flow, CO_2 concentration) are recorded by the controller of the pilot every second. Nevertheless, the raw data obtained must be corrected before it can be exploited. A correction must be applied on the analyzer to correct the pressure effect, and a correction based on the gas concentration is used for the flowmeter. The data obtained allow to determine the purity of the CO_2 obtained and the recovery of CO_2. A confidence interval for these metrics was also established based on the specifications of the equipment used.

2.3.4.1 ANALYZER CORRECTION

The gas analyzer used in the VPSA pilot (Emerson X-STREAM Enhanced) uses non-dispersive infrared (NDIR) sensor for CO_2 measurement. This type of sensor measures a signal proportional to the molecular density (Beer-Lambert law). Therefore, this density is sensitive to the temperature and pressure of measurements and must be corrected to obtain the density in the same conditions of temperature and pression as the calibration. The density can be corrected by the ideal gas law (equation 10) based on the calibration conditions [7].

$$\rho(p,T) = \rho(p_{cal},T_{cal}).\frac{p}{p_{cal}}.\frac{T_{cal}}{T} \quad (10)$$

In the case of the analyzer used in the pilot, the temperature of the device is maintained to 70°C, allowing to avoid the temperature correction. Therefore, only the pressure correction must be applied, giving the following formula (equation 11) to correct the measurement made at a pressure p to the calibration pressure p_{cal} (101325 Pa):

$$y_{CO2} = y_{CO2,measured}.\frac{1.01325}{p(bar)} \quad (11)$$

2.3.4.2 FLOW METER CORRECTION

The different flow meters and controllers used in the VPSA pilot are based on the measurement of the heat transfer rate (thermal mass flow meter) and are calibrated for a specific gas. Since the CO_2 concentration is not constant in the system, a correction must be applied to the flow measurement. This correction is based on the molar heat capacity of the measured gas and calibration gas. Equation 12 gives the theorical formula for the correction of the measured flow rate.

$$Q_{real} = Q_{measured} \cdot \frac{c_{p\,cal}(T)}{c_{p\,real}(T)} \tag{12}$$

Nevertheless, this correction method requires the temperature used for the measurement of the flow rate and is not always communicated by the manufacturers of flow meter. Instead, manufacturers give gas correction factor which needs to be applied to the measured flow rate to consider the difference of gas composition. This gas correction factor is based on the molar specific capacity calculated at the temperature of the flow measurement and is specific to a model of flow meter [8]. Equation 13 gives the formula to correct the flow rate based on the gas correction factor. If the gas measured is a mixture of n gas, a gas factor can be computed based on pure component gas factor, with P_i the percentage of gas i in the mixture (Equation 14). The gas factor given by Brooks is equal to 1 for nitrogen, and 0.74 for CO_2.

$$Q_{real} = Q_{measured} \frac{New\ gas\ factor}{Calibration\ gas\ factor} \tag{13}$$

$$Gas\ mixture\ factor = \frac{100}{\sum_i^n \frac{P_i}{gas\ factor}} \tag{14}$$

2.3.4.3 METRICS CALCULATION

Performances of VPSA pilot were evaluated by two indicators: recovery and purity. The recovery gives the percentage of CO_2 retrieved in the product stream compared to the amount of CO_2 in the feed gas. The purity is the mean purity of the CO_2 obtained at the outlet of the process.

For purity, the flow rate measured with the back pressure of the CO_2 tank, and the concentration of the gas in the tank are used for the calculation. Purity is obtained by summing the product of the flow rate measured by the back pressure (after correction) and the concentration of CO_2 tank. This sum is divided by the sum of the back pressure flow rate (equation 15).

$$Purity = \frac{\sum_{cycle} Q_{BPC\ CO_2} \cdot y_{CO_2\ tank}}{\sum_{cycle} Q_{BPC\ CO_2}} \tag{15}$$

Recovery is obtained by summing the product of the flow rate measured by the back pressure (after correction) and the concentration of CO_2 tank. This sum is divided by the sum of CO_2 flow rate measured by the CO_2 controller at the inlet of the VPSA pilot (feed section).

$$Recovery = \frac{\sum_{cycle} Q_{BPC\ CO_2} \cdot y_{CO_2\ tank}}{\sum_{cycle} Q_{feed\ CO_2}} \tag{16}$$

From equations 15 and 16, a confidence interval for purity and recovery can be determined based on the uncertainties of the devices used. The uncertainty on purity depends on the measurement of the back pressure controller, and the CO_2 concentration in the tank. The gas correction factor of the back pressure controller also depends on the CO_2 concentration. The general formula for uncertainties determination for

purity is given by the equation 17. For recovery, the uncertainty depends on the flow measured by the back pressure controller, the flow measured from the CO_2 controller in the gas generation, and the CO_2 concentration. The general formula for uncertainties determination for recovery is given by the equation 18. The detailed calculations for uncertainties are given in Appendix 5.1.1.

$$\Delta Purity = \left|\frac{\partial Purity}{\partial Q_{BPC\ CO_2\ measured}}\right| . \Delta Q_{BPC\ CO_2\ measured} + \left|\frac{\partial Purity}{\partial y_{CO2\ measured}}\right| . \Delta y_{CO_2\ measured} \quad (17)$$

$$\Delta Recovery = \left|\frac{\partial Recovery}{\partial Q_{BPC\ CO_2\ measured}}\right| . \Delta Q_{BPC\ CO_2\ measured} + \left|\frac{\partial Recovery}{\partial Q_{CO2\ measured}}\right| . \Delta y_{CO_2\ measured} + \left|\frac{\partial Recovery}{\partial Q_{CO2\ feed}}\right| . \Delta Q_{CO_2\ feed} \quad (18)$$

2.4 RESULTS OBTAINED

Three samples of MIL-160(Al) have been tested on the VPSA pilot to determine the performance of the adsorbents: MIL-160(Al) produced by MOFTECH at 3 kg scale, MIL-160(Al) produced by MOFTECH at 60 kg scale, and MIL-160(Al) produced by KRICT at 50 kg scale. All information concerning these three shaped MOFs are available in deliverable D5.1 for the first one and deliverable D6.1 for the others. Breakthrough curves have been performed for all samples at different flow rates to determine the kinetic of adsorption. For the first sample, 3-bed 5-step cycle has been tested, in addition to the 3-bed 6-step cycle. For the two other samples, only 3-bed 6-step cycle has been performed due to poor performance of the 3-bed 5-step configuration.

2.4.1 MIL-160(Al) FROM MOFTECH PRODUCED AT 3 kg SCALE

The first sample tested was provided by MOFTECH and produced in a batch of 3 kg. Since it was the first sample tested in the VPSA pilot, a larger number of tests were performed on this sample. The adsorption columns were filled each with 400 g of adsorbent. At the end of the experiments, the adsorbent was regenerated before emptying the columns, and weighed. The mass obtained was equal to 396.5 g, giving a bulk density of 375.5 $kg.m^{-3}$.

2.4.1.1 BREAKTHROUGH CURVES

Breakthrough curve measurements were performed on the sample to compare the results obtained with the previous measurements at smaller scale, and to use the results obtained for simulation. The sample was regenerated by heating at 150°C under vacuum overnight between each experiment. Eight breakthrough curves were performed with different flow rates (5, 7.5, 10 and 16.667 $NL.min^{-1}$ (*i.e.* 0.3, 0.45, 0.6 and 1 $Nm^3.h^{-1}$)), and concentrations at 5 $NL.min^{-1}$ (7, 15, 20, 30, and 50%). The pressure at the inlet of the adsorption column was measured and was equal to 1.1 bar for each breakthrough curve, excepted for the experiment made at 1 $Nm^3.h^{-1}$ where the pressure is equal to 1.5 bar. Ambient temperature was also measured. Figure 10 gives the breakthrough curves obtained, and Table 4 gives the results obtained from the experiments.

Adsorbed amount was calculated from the breakthrough curve (Equation 19 and Section 5.1.2 for uncertainties) and was compared to the value obtained by gravimetric isotherm adsorption measurement (see apparatus equipment and experimental procedure in deliverable D2.3) at the same partial pressure

and ambient temperature. The calculated adsorbed amount for the breakthrough curve at 7 and 15% of CO_2 are closed to the predicted value by the adsorption isotherms, excepted for the experiment at 1 $Nm^3.h^{-1}$. For higher CO_2 concentrations, the value obtained from breakthrough curve is under the predicted value. This can probably be explained by the heat released by the adsorbent, increasing the temperature inside the column, and reducing the adsorbed amount and by the coadsorption of nitrogen to a lesser extent.

$$q = \frac{(\sum Q_{feed} . (y_{feed} - y_{measured}))}{m_{ads}} \quad (19)$$

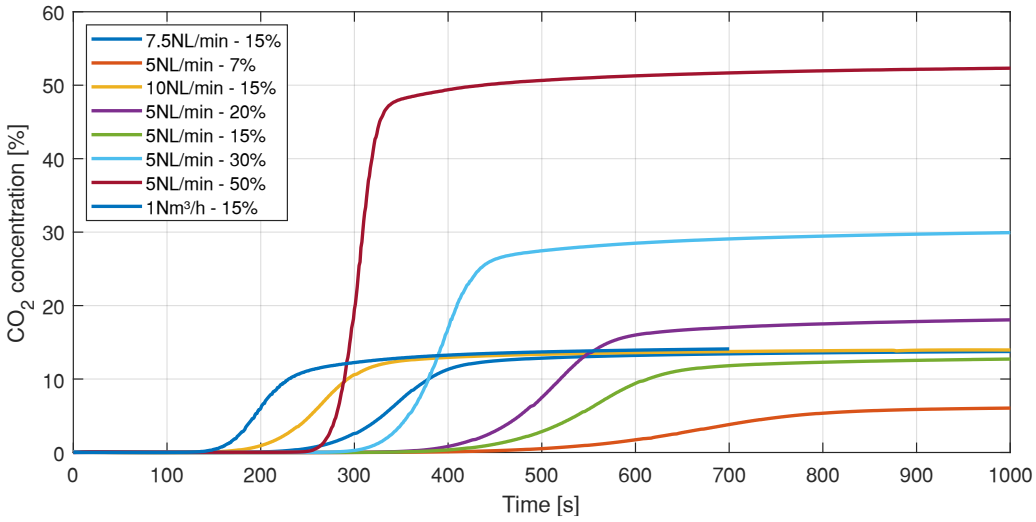

Figure 10: Breakthrough curves measured on the MIL-160(Al) from MOFTECH (3 kg scale).

Table 4: Operational conditions and results obtained for breakthrough curve measurements on MOFTECH sample produced at 3 kg scale.

Flow rate [NL.min^{-1}]	Concentration [% CO_2]	Ambient temperature [°C]	Adsorbed amount [mmol.g^{-1}]	Equilibrium adsorbed amount [mmol.g^{-1}]	Time to reach 1% [s]
7.5	15	24.6	1.25 ± 0.41	1.22	268
5	7	24.4	0.59 ± 0.24	0.64	553
10	15.2	23.1	1.33 ± 0.37	1.29	203
5	20.3	22.7	1.39 ± 0.28	1.64	408
5	14.4	22.8	1.10 ± 0.33	1.26	446
5	32.4	25.2	1.82 ± 0.42	2.11	323
5	54.9	25.5	1.99 ± 0.21	2.87	266
16.667	15.2	20.0	1.25 ± 0.10	1.53	164

2.4.1.2 3-BED 5-STEP

The 3-bed 5-step configuration was firstly tested with the adsorbent even if the results obtained from simulation (see D4.3) show that this cycle is less efficient than the 3-bed 6-step configuration (lower recovery and purity, and higher energy consumption). This cycle was the first implemented on the VPSA pilot due to its simplicity compared to the 3-bed 6-step, and to verify that the different elements of the pilot were working properly.

All the experiments were carried out with a flow rate of 1 $Nm^3.h^{-1}$ containing 15% of CO_2 and 85% of N_2. Due to a limitation of the mass flow controller of nitrogen tank, the minimal adsorption pressure is equal to 1.35 bar. It was also observed that a pressure of 0.1 bar is difficult to maintain with purge flows above 0.2 $Nm^3.h^{-1}$. All tested conditions have a blowdown pressure of 0.1 bar. Operating conditions and results obtained for the seven tested conditions are given in Table 9 in Appendix.

Generally, the system reaches its steady state after 2-3 hours of operation, which represents between 20 and 40 cycles depending on the time of the stages. The cycle is stopped when the increase of purity and recovery is less than 0.1% per cycle. The initial concentration in the nitrogen and CO_2 can influence the time needed to reach the steady state, but not the final results. As represented in Figure 11, the recoveries obtained after more than 40 cycles are similar for same cycle parameters (see experiments 2 and 3 in Table 10), but different initial concentrations in nitrogen tank.

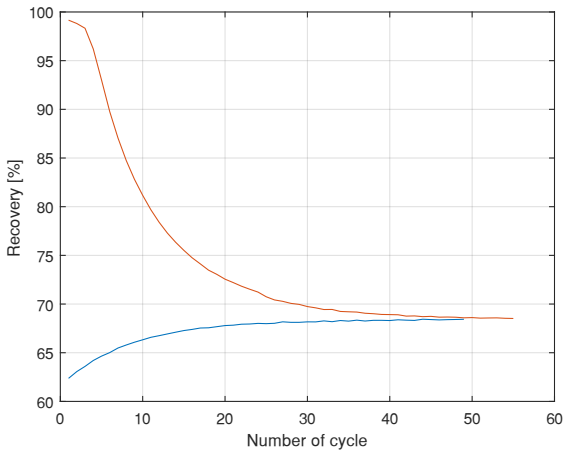

Figure 11: Evolution of recovery for two experimental measurements with the same cycle parameters (blue: start-up from previous measurement, orange: start-up from 100% N_2 in nitrogen tank).

The obtained results do not reach the targets of recovery (>90%) and purity (>95%) as expected. A relatively high purity (84.5% - experiment n°7) can be obtained with a low recovery. It is not possible to maximize both recovery and purity with this configuration. The high uncertainties obtained on recovery are due to the high flow rate measured on the back pressure controller of the CO_2 tank. The study of this cycle was not pursued to focus on the 3-bed 6-step cycle.

2.4.1.3 3-BED 6-STEP

The second configuration tested on VPSA pilot is the 3-bed 6-step cycle. The simulations carried out previously showed that this cycle made it possible to achieve the recovery and purity targets set. After preliminary tests at lower pressure (1.435 bar), the first set of experiments was performed with an adsorption pressure of 2 bar to increase the performances, and a blowdown pressure of 0.1 bar. Adsorption

time [130-180 s], purge time [65-110 s], light blowdown time [20-40 s], purge flow rate [0.1-0.3 $Nm^3.h^{-1}$] and light blowdown pressure [0.4-0.65 bar] were studied with a design of experiments. 26 experimental measurements were performed. In addition, 3 additional measurements were performed to confirm the results obtained from the design of experiments. Table 10 (Appendix) gives the 29 experimental conditions tested and the results obtained.

The results obtained were fitted to a response surface containing 21 coefficients (parameters and crossed parameters) allowing to study the effect of the parameters and predict the recovery and purity for a given condition. Figure 12 gives the actual versus predicted value obtained from the design of experiments for recovery and purity. Both fittings show a good R^2, with a value of 98.9% for recovery and 99.7% for purity.

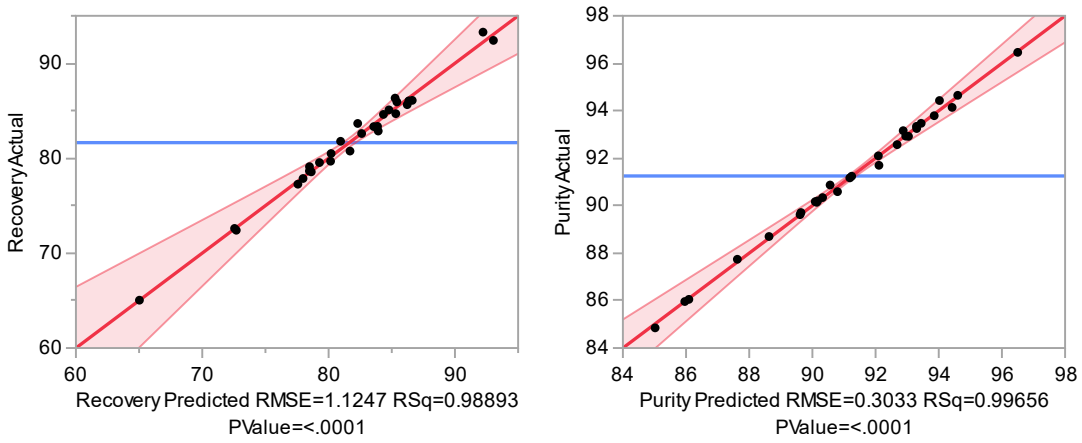

Figure 12: Actual versus predicted values for purity and recovery.

The importance of each variable was obtained by computing the sensitivity of recovery and purity to a variable by calculating the variance of the response for each variable separately. Figure 13 gives the results obtained based on the design of experiments. As represented, purge time has the most important impact on both recovery and purity, contributing to more than 50% of the result obtained. For purity, the second most important variable is adsorption time, contributing to 22% of the result obtained. Adsorption and purge time together contribute to 86% of the purity obtained. For recovery, adsorption time is less important, contributing to 14%. The second variable impacting the recovery is light blowdown time with 31% of contribution. We can observe that the cycle times are the most important contribution to the results obtained, the purge flow rate and the light blowdown pressure being less important. It is important to point out that these results are only valid in the range of values studied for the parameters.

Interaction profiles for purity and recovery were generated via the design of experiments, and are available in Figures 21 and 22 in Appendix. For purity, the figure shows that lower adsorption time gives better purity without dependency to other parameters, except for purge time where high purge time increases the effect of adsorption time. At low purge time, the purity remains constant for all adsorption time values. Best purities are obtained with high purge time without being too much influenced by the other parameters excepted for adsorption time as described above, and light blowdown time and pressure which increase the effect of purge time. The purge flow rate effect on purity has a parabolic shape, showing a maximum around 0.2 $Nm^3.h^{-1}$. This maximum is shifted to lower or higher flow rate by the other parameters. The same behavior is observed for the light blowdown pressure. Purity increases when the light blowdown time increases. The effect of this parameter is quite dependent on other parameters. High adsorption time, low

purge time, and high light blowdown pressure flatten the effect of light blowdown time. Purge flow rate seems to have no effect on this parameter.

For recovery, the effect of adsorption time is quite different. At low purge time, the best recoveries are obtained with low adsorption time, and at high purge time, the optimum is at high adsorption time. Purge flow rate and light blowdown pressure does not have a great effect on adsorption time, and low light blowdown time tends to make the effect of the adsorption time insignificant on the recovery. For purge time, the lower the time, the higher the recovery, excepted for high adsorption time and low light blowdown time where it seems to have an optimum value of purge time. The effect of purge flow rate on recovery is identical as the effect on purity. For light blowdown time and pressure, the recovery is higher with a low time and high pressure. It should be noted that when the light blowdown time is equal to 20 seconds, the pressure seems to be ineffective on recovery.

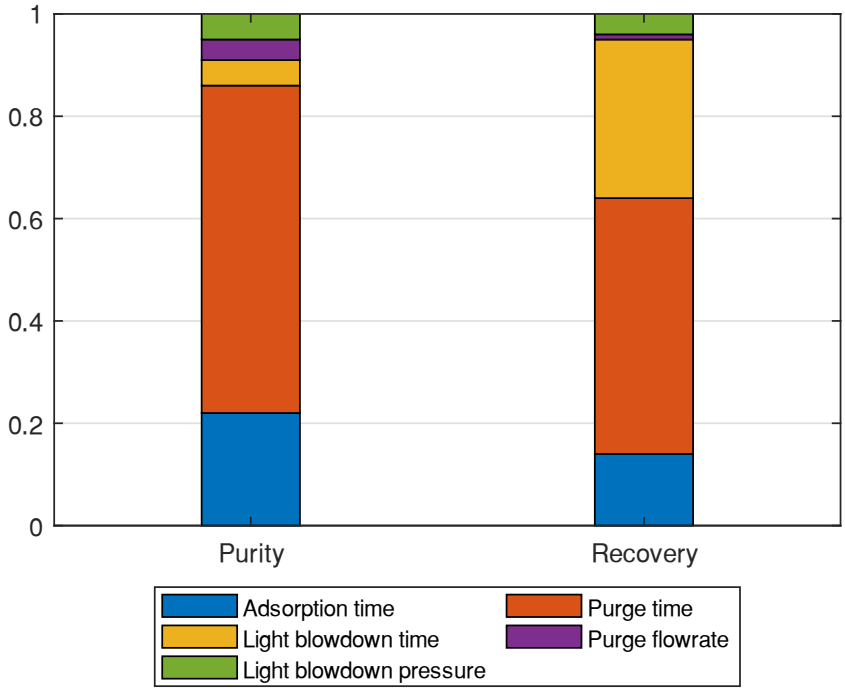

Figure 13: Impact of the five studied variables on recovery and purity for the 3-bed 6-step cycle on VPSA pilot.

Results obtained from this sample does not allow to reach the target of 95% of purity with at least 90% of recovery. The best purity obtained during the tests is 96.46%, but the recovery was equal to 65.04% (experiment 20 from Table 10 in Appendix). The best result obtained with a recovery of at least 90% is the experiment 28, giving 90.87% of purity, and 93.28% of recovery. Even if the targets of purity are not met, these results remain interesting and close to the targets. The CO_2 concentration obtained at the outlet remains high and can be used in a compression and purification unit before the storage or reuse of CO_2.

A second set of tests was made at lower adsorption pressure to find optimal conditions with a lower energy consumption. Due to a technical limitation of the nitrogen back pressure controller, the minimal adsorption pressure is equal to 1.35 bar. Adsorption time, purge time and light blowdown pressure were studied since purge flow rate and light blowdown time seems to be less important. Table 11, in Appendix, gives the experimental conditions and results obtained.

As for the 2-bar case, the results obtained from the experiments at 1.35 bar were fitted to a response surface with 6 coefficients. Obtained results show that the behavior of adsorption time, purge time, and light blowdown pressure were identical as what is said above. For recovery, adsorption time is the most

important variable, followed by purge time. For purity, purge time and light blowdown pressure are the two most important variables. The observations made with the interaction plots at 2 bar can be applied to the 1.35 bar case. Experimental measurements obtained at 1.35 bar do not allow to reach the targets of purity and recovery. The best recovery obtained at this pressure is equal to 87.71%, but only gives a purity of 61% (experiment 4 in Table 11 (Appendix)), and the best purity obtained is 86.58% with a recovery of 75.87% (experiment 2). The study of the 3-bed 6-step cycle at this pressure has not been pursued.

2.4.2 MIL-160(Al) FROM MOFTECH PRODUCED AT 60 kg SCALE

A second sample of MIL-160(Al) produced by MOFTECH was tested on the VPSA lab-pilot. Compared to the first sample, this one was produced at 60 kg scale for the industrial pilot at TCM. The 3 kg received at UMONS are an aliquot of this batch. . Adsorption isotherms measured on this sample are identical to the isotherms obtained on the sample produced at 3 kg scale. Nevertheless, bulk density of the sample is slightly higher than the previous sample, allowing to fill one column with 446 g instead of 400 g, giving a bulk density of 423 $kg.m^{-3}$ before outgassing.

Breakthrough curves and 3-bed 6-step cycle were performed on this sample. In order to reproduce conditions close to the industrial pilot, the adsorbent was not heated for regeneration since it is not possible on the industrial pilot. Instead, the adsorbent was regenerated under vacuum during two hours, and then pressurized with nitrogen before the first breakthrough curve measurement.

2.4.2.1 BREAKTHROUGH CURVES

Breakthrough curve experiments were performed on the three columns before the first cycle to evaluate the regeneration of the adsorbent. A flow rate of 0.6 $Nm^3.h^{-1}$ (10 $NL.min^{-1}$) containing 15% of CO_2 was used on the three columns, results are shown on Figure 14 . A second set of breakthrough curve measurements was performed at the same flow rate and concentration on the three columns after VPSA cycles. The goal is to see if the VPSA cycles improves the regeneration of the adsorbent. Two VPSA cycles were performed on the pilot, representing around 8 h of operation. The adsorbent was then regenerated with the same methodology as for the first breakthrough curve measurements. Results obtained are also represented on Figure 14 for comparison. In addition, Table 5 gives the adsorbed amount obtained from breakthrough curve measurements, and the time to reach 1% of CO_2 at the outlet of the column. The adsorbed amount was calculated between 0 and 3000 seconds for all curves to have a more representative comparison.

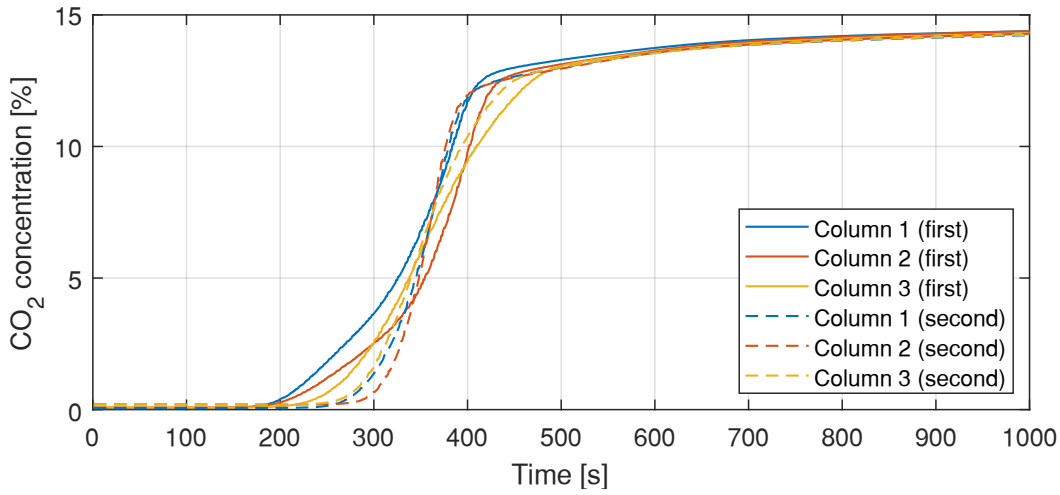

Figure 14: Breakthrough curves measured on the MIL-160(Al) from MOFTECH (60 kg scale).

The obtained curves show a more spread-out profile for the first experiments than for the second ones. This is particularly true for columns one and two, where the time to reach 1% is increased by around 70 s. An increase of adsorbed amount is observed for the three columns between the two breakthrough curves. However, the ambient temperature was lower during the second breakthrough curve measurements, increasing the equilibrium adsorbed amount. It is difficult to conclude if the increase of the adsorbed amount is caused by the temperature, or the VPSA cycles performed. A sharper profile for the second curves is also observed for the three columns. This difference can be explained by a compaction and a homogenization of the bed due to the cycles.

For the six breakthrough curves, the adsorbed amounts are lower than the equilibrium adsorbed amount from pure adsorption isotherm measurement. This difference can be explained by the co-adsorption of CO_2 and N_2 and, especially, the thermal effect inside the adsorption columns, increasing the adsorbent temperature up to 40°C, and reducing the maximum adsorbed amount. If the breakthrough curves had been carried out for a longer time, the temperature inside the column would have decreased, increasing the adsorbed amount. In order to compare the different breakthrough curves, the adsorbed quantity is calculated by integration of the breakthrough curve in 0 and 3000 s. It is possible that equilibrium is not completely reached after 3000 s and that the amount adsorbed is underestimated.

Table 5: Operational conditions and results obtained for breakthrough curve measurements on MOFTECH sample produced at 60 kg scale.

Column	Concentration [% CO_2]	Ambient temperature [°C]	Adsorbed amount [mmol.g^{-1}]	Equilibrium adsorbed amount [mmol.g^{-1}]	Time to reach 1% [s]
1 (first)	15.4	20.0	1.26±0.28	1.75	226
2 (first)	15.4	19.8	1.30±0.28	1.76	242
3 (first)	15.4	19.7	1.32±0.28	1.76	265
1 (second)	15.4	19.1	1.33±0.28	1.79	292
2 (second)	15.4	19.2	1.32±0.28	1.78	310
3 (second)	15.3	19.3	1.31±0.28	1.77	287

2.4.2.2 3-BED 6-STEP

After the breakthrough curve measurements, the performance of the adsorbent was evaluated with the 3-bed 6-step configuration. Based on the tests made on the previous sample, only an adsorption pressure of 2 bar, and a blowdown pressure of 0.1 bar were tested with this sample. The flow rate used for all the experiments was 1 $Nm^3.h^{-1}$ with a CO_2 concentration of 15%, and 85% of N_2.

As for the previous sample, a design of experiments was made to find the optimum parameters allowing to reach the targets of 90% recovery and 95% purity. Adsorption time [130-200 s], purge time [65-130 s], light blowdown time [20-40 s], purge flow rate [0.1-0.3 $Nm^3.h^{-1}$] and light blowdown pressure [0.4-0.65 bar] were studied. Initially, a lower bound of 150 s for adsorption time was chosen, according to the higher density of the material. The results obtained were not satisfactory in terms of recovery, leading to a decrease of the lower bound of this parameter. 21 experimental measurements were initially made for the design of experiments. 7 additional measurements were then tested to find the optimum and increase the accuracy of the response surface. Parameters tested and results obtained are given in Table 12 (Appendix).

As for the previous sample tested, the objectives of purity and recovery cannot be reached at the same time. The best recovery obtained is 91.6% (experiment 27 of Table 12 in Appendix) requiring a low adsorption time (130 s) and low purge time (75 s). The purity obtained is equal to 90% which is below the target but remains high enough for a compression and purification unit. It should be noted that the same parameters give a better recovery for the sample produce at 3 kg scale. The purity target can be reached with the sample produced at 60 kg scale and can reach up to 99% (experiment 9) and is obtained with a high adsorption time (200 s), low purge time (85 s), and low light blowdown pressure (0.42 bar). Unfortunately, the recovery obtained for this measurement is relatively weak: 74.5%. Several experimental conditions allow to reach a purity of at least 95%. Among these experiments, the best recovery obtained is equal to 87.6% (experiment 3) with an adsorption time of 160 s, purge time of 110 s, light blowdown time of 20 s, purge flow rate of 0.2 $Nm^3.h^{-1}$, and light blowdown pressure of 0.5 bar. The recovery obtained is close to the target, and the upper bound of the uncertainty (90.2%) is higher than the target.

Purity versus recovery obtained for both MOFs produced by MOFTECH is represented in Figure 15. For recoveries lower than 90%, the purity obtained with the adsorbent produced at 60 kg scale is higher than the 3 kg scale. For recoveries lower than 87-88 %, the purity obtained with the 60 kg scale is higher than 95%. For higher recoveries, the purity decreases sharply. The experiments 9, 3 and 26 represented in Figure 15 seem to form a circular arc (dashed dark line) representing the pareto of purity and recovery. This last assumption will have to be verified by simulation where a larger number of conditions can be tested.

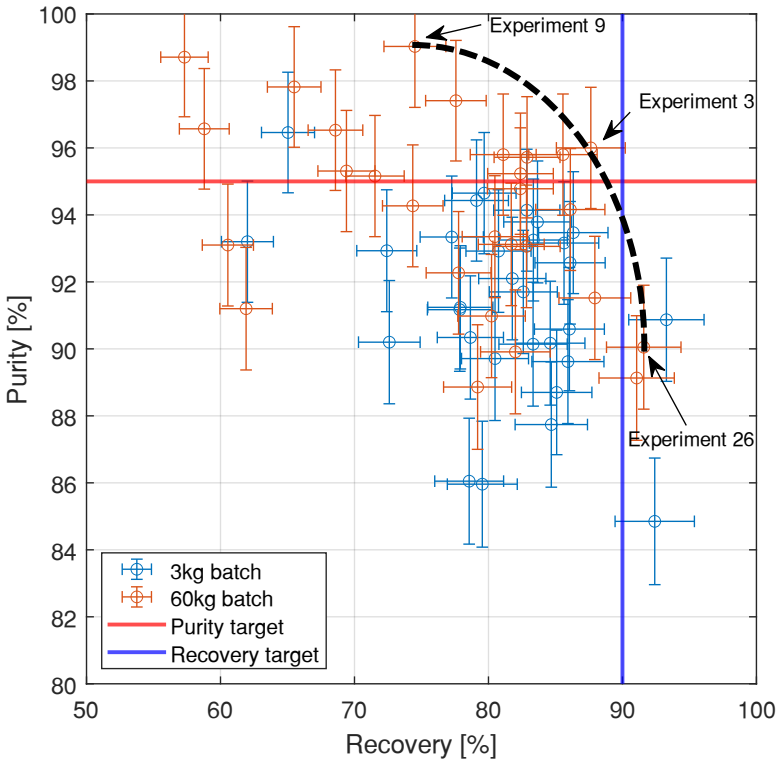

Figure 15: Purity versus recovery obtained for both MIL-160(Al) samples from MOFTECH.

2.4.3 MIL-160(Al) FROM KRICT

The third sample of MIL-160(Al) tested in the VPSA pilot was provided by KRICT and produced at 50 kg scale. The adsorption capacity of this MOF is lower than the MIL-160(Al) from MOFTECH: at a partial pressure of 0.15 bar and 20°C, the adsorbed amount of CO_2 is equal to 1.02 mmol.g^{-1} (compared to 1.32 mmol.g^{-1} for the MOFTECH samples), and the working capacity between 0.15 and 0.015 bar is equal to 0.895 mmol.g^{-1} (1.16 mmol.g^{-1} for MOFTECH).

This sample has a spherical shape, and a density higher than the sample from MOFTECH. The columns were loaded with 681 g of adsorbent before regeneration, giving a final mass of 667 g after regeneration. The average bulk density obtained is equal to 590 kg.m^{-3} (compared to 423 kg.m^{-3} for MOFTECH large scale sample) after outgassing. It should be noted that during filling, it was observed that the sample was not very homogeneous, containing a lot of dust, and agglomerated beads.

2.4.3.1 BREAKTHROUGH CURVES

Three breakthrough curves were performed to study the kinetic of the adsorbent and the adsorption capacity. The sample was regenerated by heating at 150°C under vacuum overnight between each experiment.

Three flow rates were studied for the breakthrough curves: 0.4 Nm³.h^{-1}, 0.6 Nm³.h^{-1} and 0.8 Nm³.h^{-1}. From a practical point of view, the three breakthrough curves were made on three different columns to be able to regenerate the columns at the same time. A second breakthrough curve was performed on column 1 at

0.6 $Nm^3.h^{-1}$ to check if there is an adsorbent degradation with heating. The breakthrough curves determined are represented in Figure 16, and the adsorption capacities obtained are listed in Table 6.

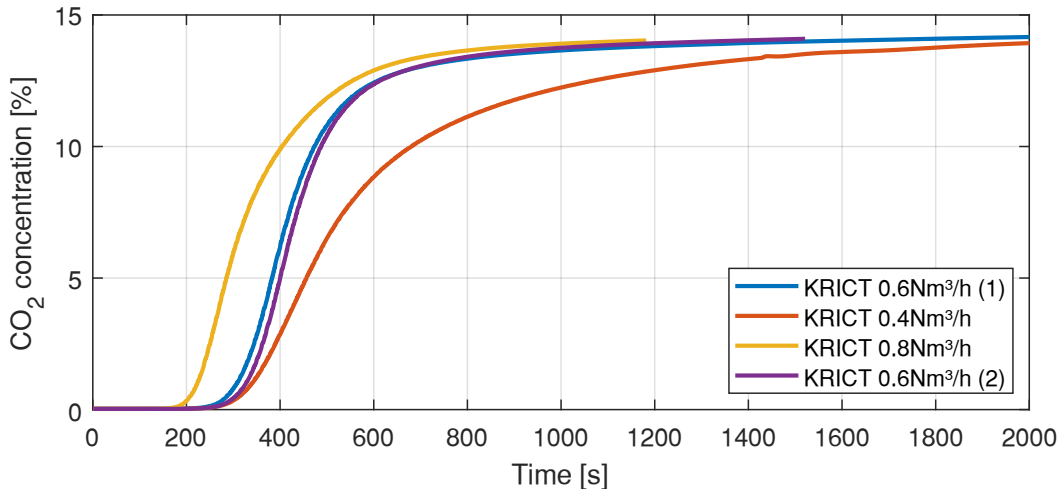

Figure 16: Breakthrough curves measured on the MIL-160(Al) from KRICT (50 kg scale).

Table 6: Operational conditions and results obtained for breakthrough curve measurements on KRICT sample.

Flow rate [$Nm^3.h^{-1}$]	Concentration [% CO_2]	Ambient temperature [°C]	Adsorbed amount [$mmol.g^{-1}$]	Equilibrium adsorbed amount [$mmol.g^{-1}$]	Time to reach 1% [s]
0.6 (1)	14.9	20	0.95±0.21	1.22	309
0.4	14.9	20	0.78±0.10	1.12	340
0.8	14.9	20	0.89±0.08	1.32	224
0.6 (2)	14.9	20.9	0.85±0.09	1.19	328

Results obtained show a higher breakthrough time compared to MOFTECH sample. We can also see that the shape of the curves is not identical between the 3 columns, showing a steeper profile for column 1 (0.6 $Nm^3.h^{-1}$), and a more spread-out profile for 0.4 and 0.8 $Nm^3.h^{-1}$ curves. This can be explained by the difference of density between the three columns, but also by the inhomogeneity of the sample. The two measurements performed at 0.6 $Nm^3.h^{-1}$ are similar and no significant degradation in terms of capacity is observed.

The breakthrough curves obtained from KRICT sample and MOFTECH samples (3 kg and 60 kg scale) are represented together in Figure 17 for a flow rate of 0.6 $Nm^3.h^{-1}$ and 15% CO_2. As the density increases, the breakthrough time increases as observed for the two samples of MOFTECH. Even if the adsorption capacity of the KRICT sample is lower, the higher density results in a longer breakthrough time. For the two samples from MOFTECH, the beginning of the curves is identical, but differs towards the end. A break is observed in the curve obtained with the sample made at 60 kg scale. This shape is probably due to the higher density, leading to an increase of thermal effects in the adsorption column. For the KRICT sample, the profile is more spread out, maybe due to thermal effects, or the binder used.

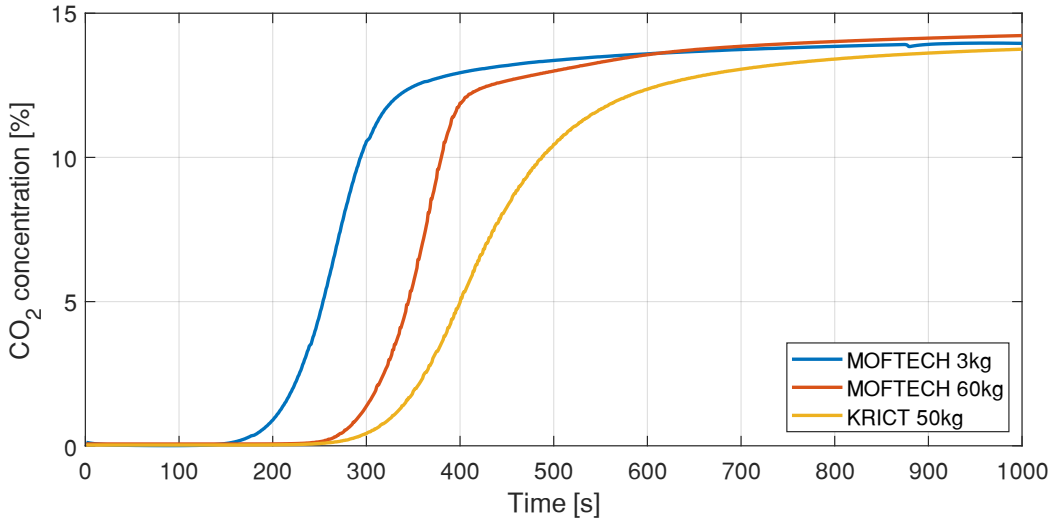

Figure 17: Comparison of breakthrough curves measured on the three samples of MIL-160(Al) at 0.6 $Nm^3.h^{-1}$ and 15% CO_2.

2.4.3.2 3-BED 6-STEP

The results obtained on the MOFTECH sample have shown that only the 3-bed 6-step cycle can reach the targets of recovery and purity. In addition, only an adsorption pressure of 2 bar allows to reach 90% of recovery. Based on these results, only 5 experimental measurements have been done with this sample. Table 13 (Appendix) gives the experimental conditions tested for an adsorption pressure of 2 bar, and a blowdown pressure of 0.1 bar.

Even if the breakthrough time of the KRICT sample is higher, the recoveries obtained are lower than the MOFTECH sample. This can come from slower adsorption kinetic, or the non-homogeneity of the particles. The performances obtained are very close to the MOFTECH sample. A more detailed study of this sample should be carried out on the industrial pilot.

3 CONCLUSIONS

A fully instrumented and automated laboratory vacuum pressure swing adsorption pilot (VPSA) was successfully developed. The pilot allows to test different materials and process configurations with different gas conditions (CO_2 concentration, flow rate, dry or wet …). With this pilot, other adsorbents or other VPSA process configurations can also be tested at laboratory scale.

The performances for CO_2 capture of MIL-160(Al) produced by MOFTECH and KRICT in a 3-bed 6-step VPSA have been studied within the lab pilot. The impacts of operating parameters (adsorption time, purge time, purge flow rate, light blowdown time, light blowdown pressure, …) were assessed, allowing a better understanding of the process. For the three samples, the effects of the parameters are similar, and the results obtained for a set of parameters are close for the three MOFs. Recoveries and purities obtained with the MOF produced by MOFTECH are closed to the targets. Both targets are not fully met, but some sets of parameters give purity higher than 95% and a recovery close to 90%. The optimum conditions can be refined with simulations.

Results obtained from VPSA lab-pilot will be used to refine the simulations models developed in D4.3. Thanks to the numerous recordings of the laboratory pilot, some uncertain parameters (heat transfer coefficients, kinetics, …) will be adjusted to fit the experimental results. In addition, the results of the VPSA lab-pilot will allow to determine the optimum conditions of the industrial VPSA pilots. The results obtained on a laboratory and industrial scales could be compared to determine if the performances of the process remain the same during the upscaling of the process.

In addition to the work done, a second adsorbent will be tested on the laboratory VPSA pilot. MIL-120(Al) produced at medium scale in Task 5.1 will be tested before its possible use in the industrial pilot, as for the MIL-160(Al). For MIL-160(Al), other flue gas conditions can be tested on the pilot to find the optimum operating conditions in the range of 5 to 20% CO_2. The influence of water in the flue gas can also be tested to determine if there is a loss of performances compared to the dry conditions.

4 REFERENCES

[1] J. N. Tilton, “Fluid and Particle Dynamics,” in *Perry’s Chemical Engineers’ Handbook*, 8th editio., D. W. Green, Ed. McGraw-Hill, 2008.

[2] S. W. Churchill, “Friction Factor Equation Spans All Fluid Flow Regimes,” *Chem. Eng.*, vol. 84, pp. 91–92, 1977.

[3] C. Co., “Flow of Fluids through Valves, Fittings, and Pipe,” 1969.

[4] R. Byron Bird, W. E. Stewart, and E. N. Lightfoot, *Transport Phenoma*, Second Edi. New York, 2002.

[5] A. Roth, *Vacuum technology*, Third Edit. 1990.

[6] J. G. Ziegler and N. B. Nichols, “Optimum settings for automatic controllers,” *Trans. Am. Soc. Mech. Eng.*, vol. 64, no. 8, pp. 759–765, 1942.

[7] M. Marinov, G. Nikolov, E. Gieva, and B. Ganev, “Improvement of NDIR carbon dioxide sensor accuracy,” *Proc. Int. Spring Semin. Electron. Technol.*, vol. 2015-September, pp. 466–471, 2015, doi: 10.1109/ISSE.2015.7248042.

[8] S. A. Tison, “A critical evaluation of thermal mass flow meters,” *J. Vac. Sci. Technol. A Vacuum, Surfaces, Film.*, vol. 14, no. 4, pp. 2582–2591, 1996, doi: 10.1116/1.579985.

5 APPENDIX

5.1 UNCERTAINTIES CALCULATION

5.1.1 RECOVERY AND PURITY

$$Purity = \frac{\sum_{cycle} Q_{BPC\ CO_2\ measured} \cdot \left(\frac{1}{\frac{0.26}{0.74} y_{CO2} + 1} \right) y_{CO_2\ tank}}{\sum_{cycle} Q_{BPC\ CO_2\ measured} \cdot \left(\frac{1}{\frac{0.26}{0.74} y_{CO2} + 1} \right)} \quad (20)$$

The purity formula must be derived according to the flow rate and CO_2 concentration measured.

$$\left| \frac{\partial Purity}{\partial Q_{BPC\ CO_2\ measured}} \right| = \frac{\Sigma_{cycle} \left(\left(\frac{1}{\frac{0.26}{0.74} y + 1} \right) y_{CO_2} \right) \cdot \Sigma_{cycle} \left(Q \cdot \left(\frac{1}{\frac{0.26}{0.74} y + 1} \right) \right) - \Sigma_{cycle} \left(Q \left(\frac{1}{\frac{0.26}{0.74} y + 1} \right) y \right) \cdot \Sigma_{cycle} \left(\left(\frac{1}{\frac{0.26}{0.74} y + 1} \right) \right)}{\left(\Sigma_{cycle} \left(Q \cdot \left(\frac{1}{\frac{0.26}{0.74} y + 1} \right) \right) \right)^2} \quad (21)$$

$$\left| \frac{\partial Purity}{\partial y_{CO_2\ measured}} \right| = \frac{\Sigma_{cycle} \left(Q \cdot \frac{\left(\frac{0.26}{0.74} + 1 \right) - y \left(\frac{0.26}{0.74} \right)}{\left(\frac{0.26}{0.74} y + 1 \right)^2} \right) \cdot \Sigma_{cycle} \left(Q \cdot \left(\frac{1}{\frac{0.26}{0.74} y + 1} \right) \right) - \Sigma_{cycle} \left(Q \left(\frac{1}{\frac{0.26}{0.74} y + 1} \right) y \right) \cdot \Sigma_{cycle} \left(-Q \frac{\frac{0.26}{0.74}}{\left(\frac{0.26}{0.74} y + 1 \right)^2} \right)}{\left(\Sigma_{cycle} \left(Q \cdot \left(\frac{1}{\frac{0.26}{0.74} y + 1} \right) \right) \right)^2} \quad (22)$$

The accuracy of the back pressure controller ($\Delta Q_{BPC\ CO_2\ measured}$) is equal to 1% of the full scale (which is 0.2 $Nm^3.h^{-1}$). The accuracy of the analyzer is equal to 1% of the full scale plus 0.5% of the full scale if a flow

is present. The pressure also adds 0.01% of uncertainties related to the measurement, per hPa of difference compared to the calibration reference.

The same methodology can be applied to the recovery calculation. The complete formula of recovery is given by equation 23.

$$Recovery = \frac{\sum_{cycle} Q_{BPC\ CO_2\ measured} \cdot \left(\frac{1}{\frac{\frac{0.26}{0.74} y_{CO2} + 1}{0.74}} \right) y_{CO_2\ tank}}{\sum_{cycle} Q_{CO_2\ feed}} \quad (23)$$

The different derivates can be calculated, giving the following formulas:

$$\frac{\partial Recovery}{\partial Q_{BPC\ CO_2\ measured}} = \frac{\sum_{cycle} \left(\frac{1}{\frac{\frac{0.26}{0.74} y_{CO2} + 1}{0.74}} \right) y_{CO_2\ tank}}{\sum_{cycle} Q_{CO_2\ feed}} \quad (24)$$

$$\frac{\partial Recovery}{\partial y_{CO2\ measured}} = \frac{\sum_{cycle} \left(Q_{BPC} \cdot \frac{\left(\frac{0.26}{0.74} + 1\right) - y\left(\frac{0.26}{0.74}\right)}{\left(\frac{0.26}{0.74} y + 1\right)^2} \right)}{\sum_{cycle} Q_{CO_2\ feed}} \quad (25)$$

$$\frac{\partial Recovery}{\partial Q_{CO2\ feed}} = \frac{-\sum_{cycle} Q_{BPC} \cdot \left(\frac{1}{\frac{\frac{0.26}{0.74} y_{CO2} + 1}{0.74}} \right) y_{CO_2\ tank}}{\left(\sum_{cycle} Q_{CO_2\ feed}\right)^2} \quad (26)$$

The accuracy of the flow controller used for gas generation ($\Delta Q_{CO_2\ feed}$) is equal to 0.5% of the read value, plus 0.1% of the full scale (1 $Nm^3.h^{-1}$).

5.1.2 ADSORBED AMOUNT FROM BREAKTHROUGH CURVE

The calculation of the adsorbed amount from breakthrough curve can be rewritten as the following formula:

$$q = \frac{\left(\sum Q_{CO_2\ feed} - y_{measured}\left(Q_{CO_2\ feed} + Q_{N_2\ feed}\right)\right)}{m_{ads}} \quad (27)$$

The uncertainty can be obtained by calculating the derivate of this formula according to the measured variables:

$$\Delta q = \left|\frac{\partial q}{\partial Q_{CO_2\ feed}}\right| \Delta Q_{CO_2}\ feed + \left|\frac{\partial q}{\partial Q_{n_2\ feed}}\right| \Delta Q_{N_2}\ feed + \left|\frac{\partial q}{\partial y_{measured}}\right| \Delta y_{measured} + \left|\frac{\partial q}{\partial m_{ads}}\right| \Delta m_{ads} \quad (28)$$

$$\Delta q = \frac{|\sum 1 - y|}{m_{ads}} \Delta Q_{CO_2} + \frac{|\sum -y|}{m_{ads}} \Delta Q_{N_2} + \frac{|\sum (Q_{CO2} + Q_{N2})|}{m_{ads}} \Delta y + \frac{\left|-\sum Q_{CO_2} - y\left(Q_{CO_2} + Q_{N_2}\right)\right|}{(m_{ads})^2} \Delta m \quad (29)$$

The uncertainties for the concentration measured and the flow rate of CO_2 are similar to recovery and purity calculations (Section 5.1.1). For the nitrogen flow rate, the uncertainty is equal to 0.5% of the value read, plus 0.1% of the full scale. The uncertainty on the mass of adsorbent is equal to 0.2 g.

5.2 VPSA P&ID

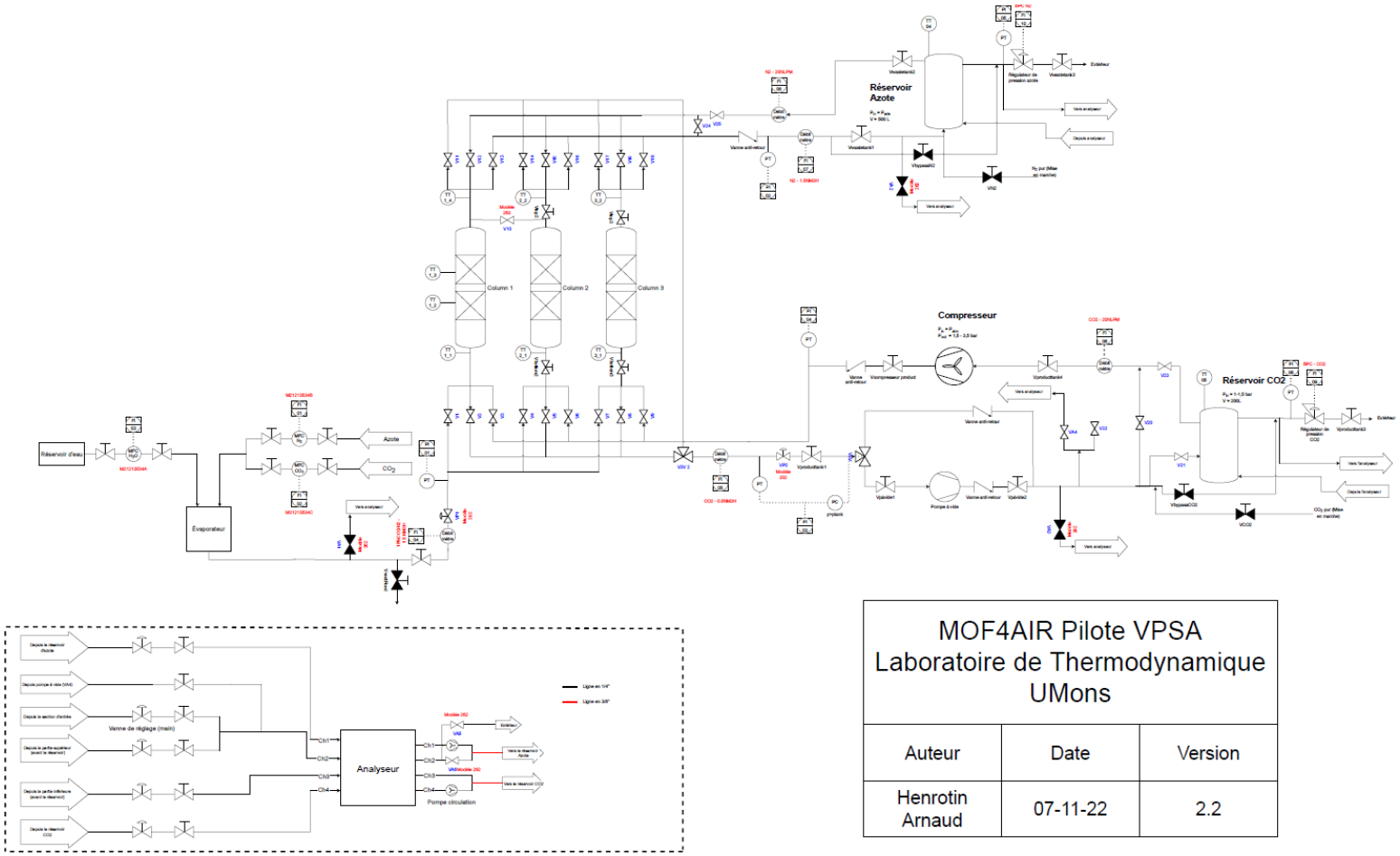

Figure 18: Complete P&ID of the VPSA pilot.

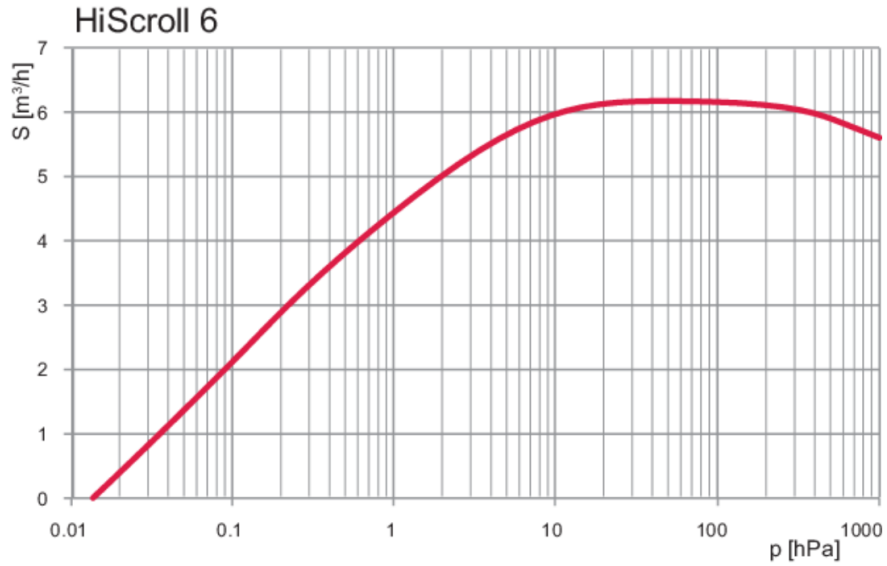

Figure 19: Characteristic curve of the HiScroll 6 vacuum pump.

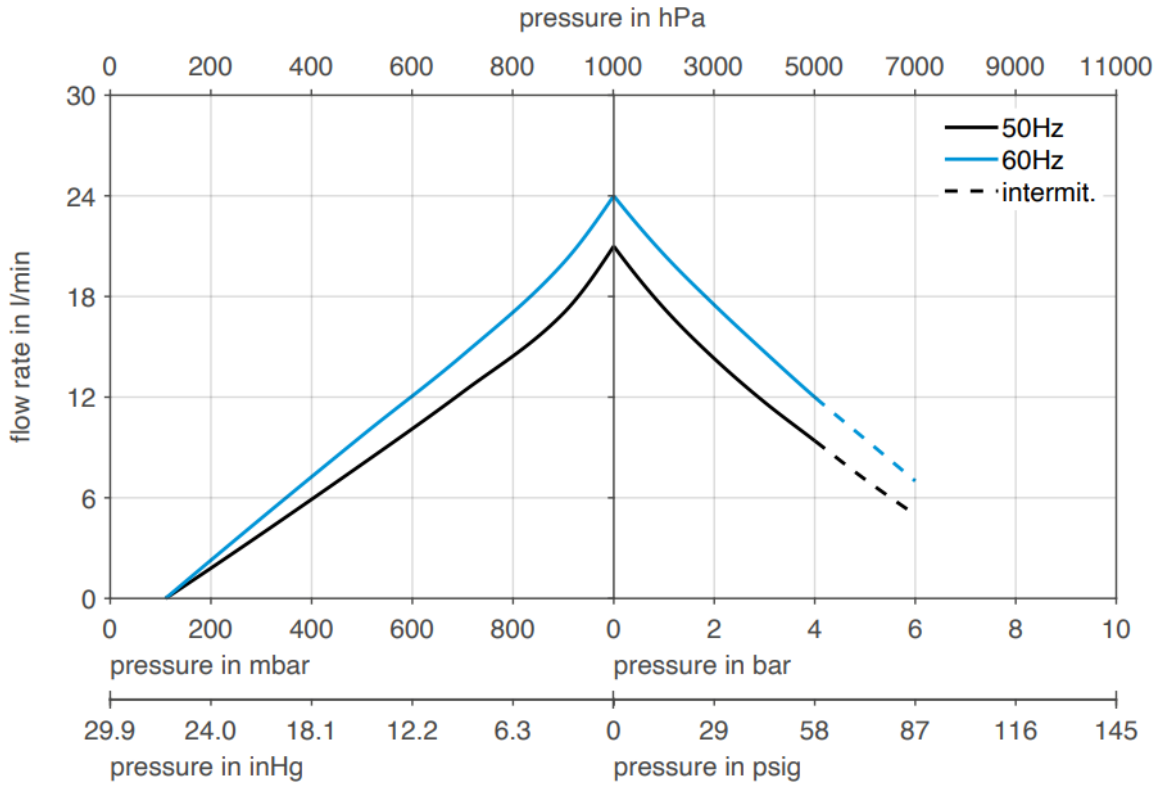

Figure 20: Characteristic curve of the N922STE diaphragm pump.

Table 7: Valve set used for the 3-bed 5-step cycle (the valves not specified are equal to 0 for each step).

Step	1	2	3	4	5	6	7	8	9
V1	1	0	0	0	0	0	1	1	1
V2	0	0	1	1	1	1	0	0	0
V3	0	1	0	0	0	0	0	0	0
V4	1	1	1	1	0	0	0	0	0
V5	0	0	0	0	0	1	1	1	1
V6	0	0	0	0	1	0	0	0	0
V7	0	0	0	1	1	1	1	0	0
V8	1	1	1	0	0	0	0	0	1
V9	0	0	0	0	0	0	0	1	0
V12	0	0	0	0	0	1	0	0	0
V13	1	1	0	0	0	0	0	1	1
V15	0	0	0	0	0	0	0	0	1
V16	0	1	1	1	1	0	0	0	0
V18	0	0	1	0	0	0	0	0	0
V19	0	0	0	0	1	1	1	1	0
V21	1	1	1	1	1	1	1	1	1
V23	0	1	0	0	1	0	0	1	0
V25	0	0	1	0	0	1	0	0	1
MFC N2	0	0	1	0	0	1	0	0	1
MFC CO2	0	1	0	0	1	0	0	1	0
Vacuum pump	1	1	1	1	1	1	1	1	1
Compressor	0	1	0	0	1	0	0	1	0

Table 8: Valve set used for the 3-bed 6-step cycle (the valves not specified are equal to 0 for each step).

	1	2	3	4	5	6	7	8	9
V1	1	1	1	0	0	0	0	0	0
V2	0	0	0	0	0	1	1	0	0
V3	0	0	0	1	0	0	0	0	0
V4	0	0	0	1	1	1	0	0	0
V5	1	0	0	0	0	0	0	0	1
V6	0	0	0	0	0	0	1	0	0
V7	0	0	0	0	0	0	1	1	1
V8	0	0	1	1	0	0	0	0	0
V9	1	0	0	0	0	0	0	0	0
V11	0	0	0	0	1	0	0	0	0
V12	0	0	0	0	0	0	1	1	1
V13	1	1	1	1	0	0	0	0	0
V14	0	0	0	0	0	0	0	1	0
V15	1	1	1	0	0	0	0	0	0
V16	0	0	0	1	1	1	1	0	0
V17	0	1	0	0	0	0	0	0	0
V18	0	0	0	1	1	1	0	0	0
V19	1	0	0	0	0	0	1	1	1
V20	1	0	0	1	0	0	1	0	0
V21	0	0	1	0	0	1	0	0	1
V22	0	1	0	0	1	0	0	1	0
V24	1	1	1	1	1	1	1	1	1
V3V2	1	0	1	1	0	1	1	0	1
MFC N2	1	1	1	1	1	1	1	1	1
MFC CO2	1	0	0	1	0	0	1	0	0
Vacuum pump	1	1	1	1	1	1	1	1	1
Compressor	1	0	0	1	0	0	1	0	0

Table 9: Parameters tested with the 3-bed 5-step cycle.

N°	Adsorption time [s]	Purge time [s]	Rinse time [s]	Purge flow rate [$Nm^3.h^{-1}$]	Rinse flow rate [$Nm^3.h^{-1}$]	Adsorption pressure [bar]	Purity [%]	Recovery [%]
1	114	10	94	0.54	0.05	1.7	53.64 ± 2.09	30.94 ± 1.56
2	114	30	64	0.54	0.1	1.4	44.95 ± 2.2	70.55 ± 4.14
3	114	30	64	0.54	0.1	1.35	43.59 ± 2.2	69.03 ± 4.14
4	60	40	10	0.2	0.05	1.35	40.17 ± 2.33	77.38 ± 5.2
5	60	40	10	0.2	0.05	1.35	40.78 ± 2.34	78.34 ± 5.21
6	160	40	40	0.05	0.05	1.4	68.39 ± 1.97	38.44 ± 1.62
7	160	40	30	0.05	0.5	1.4	84.54 ± 1.95	45.36 ± 1.67

Table 10: Parameters tested with the 3-bed 6-step cycle (MOFTECH sample 3 kg scale) with an adsorption pressure of 2 bar.

N°	Adsorption time [s]	Purge time [s]	Light blowdown time [s]	Purge flow rate [$Nm^3.h^{-1}$]	Light blowdown pressure [bar]	Purity [%]	Recovery [%]
1	130	65	30	0.2	0.5	90.59 ± 1.84	86.04 ± 2.61
2	170	100	30	0.2	0.65	92.1 ± 1.83	81.78 ± 2.51
3	170	100	30	0.3	0.65	91.17 ± 1.84	77.86 ± 2.42
4	170	70	30	0.2	0.65	87.74 ± 1.87	84.69 ± 2.7
5	130	65	30	0.3	0.5	90.17 ± 1.85	84.61 ± 2.59
6	130	65	30	0.1	0.5	88.7 ± 1.86	85.09 ± 2.63
7	150	65	40	0.2	0.5	89.71 ± 1.85	80.49 ± 2.5

8	130	65	30	0.2	0.4	90.14 ± 1.85	83.33 ± 2.55
9	150	85	30	0.2	0.5	92.92 ± 1.83	80.75 ± 2.43
10	170	85	30	0.2	0.65	89.62 ± 1.85	85.93 ± 2.69
11	170	85	30	0.2	0.5	91.7 ± 1.84	82.6 ± 2.54
12	170	100	30	0.25	0.5	93.34 ± 1.82	77.26 ± 2.36
13	170	100	20	0.2	0.5	93.16 ± 1.83	85.64 ± 2.59
14	180	100	20	0.2	0.5	92.57 ± 1.83	86.09 ± 2.62
15	180	110	20	0.2	0.5	93.25 ± 1.82	83.35 ± 2.54
16	170	100	30	0.2	0.5	94.43 ± 1.81	79.11 ± 2.38
17	170	110	20	0.2	0.5	93.79 ± 1.82	83.66 ± 2.52
18	160	100	20	0.2	0.5	93.47 ± 1.82	86.33 ± 2.59
19	180	65	20	0.3	0.4	90.34 ± 1.84	78.65 ± 2.47
20	180	110	40	0.1	0.4	96.46 ± 1.8	65.04 ± 1.98
21	180	65	20	0.1	0.65	85.96 ± 1.88	79.54 ± 2.61
22	130	65	20	0.1	0.65	84.85 ± 1.89	92.41 ± 2.96
23	180	65	40	0.1	0.4	90.20 ± 1.84	72.60 ± 2.30
24	180	65	40	0.3	0.65	86.05 ± 1.88	78.56 ± 2.57
25	180	110	40	0.1	0.65	92.93 ± 1.82	72.41 ± 2.24
26	180	65	20	0.1	0.4	91.24 ± 1.84	77.9 ± 2.43
27	160	110	20	0.17	0.58	94.65 ± 1.81	79.68 ± 2.38

28	130	75	20	0.15	0.6	90.87 ± 1.84	93.28 ± 2.81
29	150	100	20	0.21	0.56	94.14 ± 1.82	82.86 ± 2.47

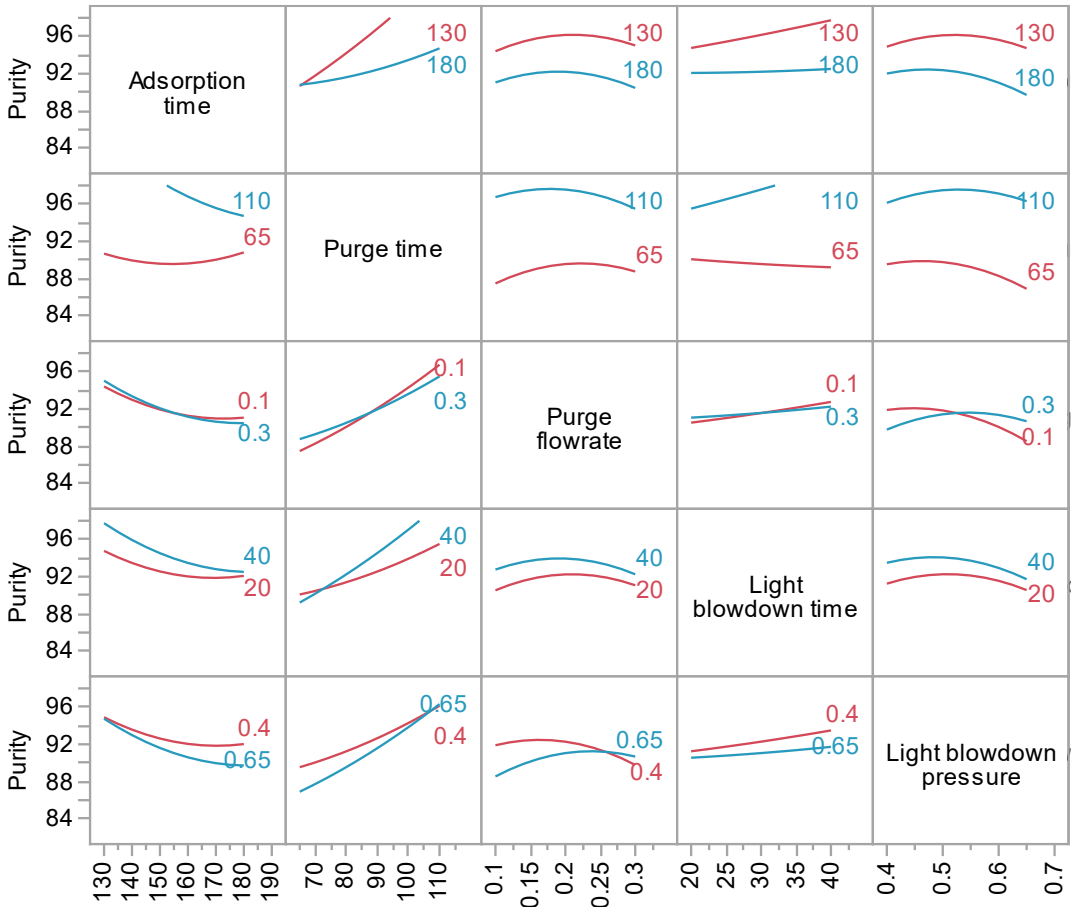

Figure 21: Interaction profiles for purity.

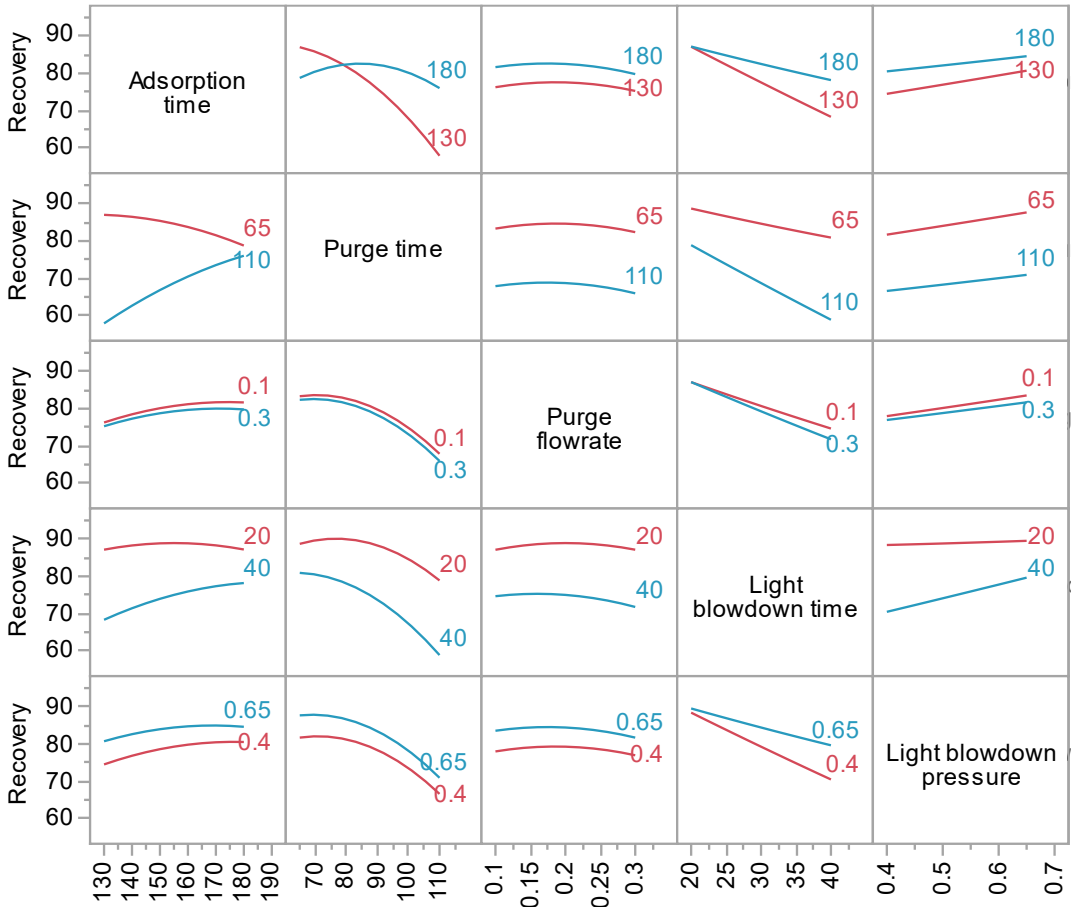

Figure 22: Interaction profiles for recovery.

Table 11: Parameters tested with the 3-bed 6-step cycle (MOFTECH sample 3 kg scale) with an adsorption pressure of 1.35 bar.

N°	Adsorption time [s]	Purge time [s]	Light blowdown pressure [bar]	Purity [%]	Recovery [%]
1	120	65	0.5	86.08 ± 1.88	80.86 ± 2.57
2	160	100	0.65	86.58 ± 1.87	75.87 ± 2.46
3	80	30	0.5	74.82 ± 1.96	84.32 ± 2.99
4	80	30	0.8	61 ± 2.07	87.71 ± 3.78
5	160	30	0.8	67.56 ± 2.02	61.92 ± 2.52
6	120	65	0.8	73.17 ± 1.98	85.4 ± 3.14
7	160	100	0.65	82.68 ± 1.9	77.34 ± 2.6
8	160	30	0.5	78.89 ± 1.93	59.75 ± 2.14

Table 12: Parameters tested with the 3-bed 6-step cycle (MOFTECH sample 60 kg scale) with an adsorption pressure of 2 bar.

N°	Adsorption time [s]	Purge time [s]	Light blowdown time [s]	Purge flow rate [$Nm^3.h^{-1}$]	Light blowdown pressure [bar]	Purity [%]	Recovery [%]
1	150	100	20	0.21	0.56	94.16 ± 1.82	86.11 ± 2.58
2	160	110	20	0.17	0.58	94.78 ± 1.82	82.38 ± 2.46
3	160	100	20	0.2	0.5	96.0 ± 1.81	87.64 ± 2.57
4	180	110	20	0.2	0.5	95.8 ± 1.81	85.56 ± 2.55
5	200	92	40	0.23	0.65	89.91 ± 1.85	82.01 ± 2.6
6	180	120	29	0.1	0.4	97.82 ± 1.8	65.50 ± 2.0
7	200	130	20	0.16	0.42	95.8 ± 1.81	81.1 ± 2.46
8	200	121	33	0.3	0.4	98.71 ± 1.78	57.31 ± 1.77
9	200	85	22	0.3	0.42	99.03 ± 1.82	74.51 ± 2.31
10	150	92	28	0.21	0.4	96.53 ± 1.8	68.58 ± 2.04
11	190	107	20	0.3	0.65	90.98 ± 1.84	80.23 ± 2.52
12	162	96	36	0.12	0.65	94.27 ± 1.82	74.35 ± 2.26
13	170	85	27	0.27	0.56	93.06 ± 1.83	82.84 ± 2.51
14	172	103	39	0.3	0.51	93.1 ± 1.82	60.55 ± 1.91
15	185	130	25	0.1	0.65	95.31 ± 1.81	69.4 ± 2.13
16	182	85	40	0.1	0.4	95.16 ± 1.81	71.53 ± 2.18
17	197	105	29	0.1	0.54	92.27 ± 1.83	77.77 ± 2.42

18	200	85	20	0.17	0.65	88.86 ± 1.86	79.19 ± 2.54
19	200	130	40	0.1	0.55	96.57 ± 1.8	58.79 ± 1.86
20	167	85	20	0.13	0.4	95.23 ± 1.81	82.39 ± 2.45
21	172	121	21	0.3	0.46	91.2 ± 1.83	61.91 ± 1.96
22	150	98	20	0.1	0.46	97.41 ± 1.8	77.57 ± 2.26
23	180	85	20	0.3	0.4	93.35 ± 1.82	80.48 ± 2.44
24	170	94	20	0.2	0.5	95.72 ± 1.81	82.88 ± 2.46
25	160	90	20	0.2	0.6	91.52 ± 1.84	87.94 ± 2.68
26	150	100	20	0.2	0.65	93.12 ± 1.83	81.7 ± 2.46
27	130	75	20	0.15	0.6	90.05 ± 1.85	91.59 ± 2.78
28	145	75	20	0.23	0.6	89.13 ± 1.86	91.06 ± 2.81

Table 13: Parameters tested with the 3-bed 6-step cycle (KRICT sample 50 kg scale) with an adsorption pressure of 2 bar.

N°	Adsorption time [s]	Purge time [s]	Light blowdown time [s]	Purge flow rate [$Nm^3.h^{-1}$]	Light blowdown pressure [bar]	Purity [%]	Recovery [%]
1	150	100	20	0.21	0.56	95.07 ± 1.85	82.41 ± 2.55
2	130	75	20	0.15	0.6	85.49 ± 1.88	94.8 ± 3
3	170	100	30	0.2	0.5	90.34 ± 1.85	82.69 ± 2.58
4	160	100	20	0.2	0.5	92.7 ± 1.83	86.8 ± 2.63
5	160	110	20	0.17	0.58	94.71 ± 1.82	81.61 ± 2.44